Synthesis and evaluation of a monitoring and control system for a neutron monitor

R Fuchs

24177393

Dissertation submitted in partial fulfilment of the requirements for the degree *Magister in Computer and Electronic Engineering* at the Potchefstroom Campus of the North-West University

Supervisor: Prof J.E.W Holm

Co supervisor Prof H. Moraal

April 2014

ACKNOWLEDGEMENTS

Soli Deo Gloria

"To God alone the glory"

ACKNOWLEDGEMENTS

I would further like to thank the following people for their contributions throughout, and for making this project a success:

- My supervisor, Prof. J.E.W. Holm, for the extraordinary way in which he guided me through his expert advice and support;
- Prof. H. Moraal, for the opportunities, guidance and support, especially in the field of physics;
- SANAP, the NRF and the North-West University for the necessary funding to complete this project;
- Ruan Nel for his support and advice on the project especially during the production phase and CAD modelling;
- All my colleagues at the CSR for their logistical support;
- Liezel Tait, for her love, understanding and support; and finally
- my family and friends for their inputs, support and motivation.

SUMMARY

SYNTHESIS AND EVALUATION OF A MONITORING AND CONTROL SYSTEM FOR A NEUTRON MONITOR

Neutron monitors detect secondary particles produced by the collision of cosmic rays and atmospheric nuclei. The need exists for a mini-neutron monitor data acquisition system (MNM-DAS) to replace the existing recording system of the calibration neutron monitor developed in 2003 at the North-West University Centre for Space Research. The MNM-DAS must also replace the recording system of a standard NM64 neutron monitor.

This research thus includes the development of the MNM-DAS using Design Science Research (DSR) in conjunction with Systems Engineering (SE) to streamline the design phase and maximize research output. A literature study is conducted, where an overview of the calibration monitor system is provided, together with the objectives for the development of the MNM system.

An abstract system architecture was drawn up in the conceptual design phase of the project to provide a coherent description of all system functions. The system architecture was derived for the existing system, including additional functions of the required system, by performing a functional analysis. The architecture describes the function and fit of each functional unit and all interfaces that form an integrated system.

From the conceptual design and system architecture, a preliminary synthesis was done. Following the preliminary synthesis, electronic circuitry was developed to capture the arrival time of pulses from the proportional neutron monitor counter tubes along with environmental variables, such as temperature, pressure, and location, which all influence the count rate.

The MNM-DAS was successfully designed and developed by following this Systems-Engineering approach embedded into a Design Science Research framework. The MNM-DAS was constructed and tested, and is currently being used to provide neutron count data in real-world applications internationally.

Keywords: Neutron monitor, design science research, calibration monitor

OPSOMMING

ONTWERP EN EVALUERING VAN ‘N REGISTRASIESTELSEL VIR ‘N NEUTRONMONITOR

Neutronmonitors registreer sekondêre deeltjies wat deur die botsing van kosmiese strale en atmosferiese kerne geproduseer word. Daar is ‘n behoefte aan ‘n mini-neutronmonitor dataverkrygingstelsel (MNM-DAS) om die bestaande optekeningstelsel van die kalibrasie neutronmonitor wat in 2003 by die Noordwes-Universiteit se Ruimtenavorsingsentrum gebou is te vervang. Die MNM-DAS moet ook die optekeningstelsel van ‘n standaard NM64 neutronmonitor vervang.

Hierdie navorsing het dus gekyk na die ontwikkeling van die MNM-DAS met die gebruik van Design Science Research (DSR) in samehang met stelselsingenieurswese (SI) om die ontwerpfase te vaartbelyn en om navorsingsuitsette te optimeer. ‘n Literatuurstudie is onderneem, waar ‘n oorsig van die kalibrasie-moniteerstelsel voorsien is, sowel as die doelwitte vir die ontwikkeling van die MNM-stelsel.

‘n Abstrakte stelselargitektuur is opgestel in die konseptuele ontwerpfase van die projek om ‘n koherente beskrywing van al die stelselfunksies te verskaf. Die stelselargitektuur is afgelei van die bestaande stelsel, en sluit addisionele funksies van die verlangde stelsel in deur die uitvoering van ‘n funksionele analise. Die argitektuur beskryf die funksie en passing van elke funksionele eenheid en al die koppelvlakke wat saam ‘n geïntegreerde stelsel vorm.

Uit die konseptuele ontwerp en die stelselargitektuur is ‘n voorlopige sintese gedoen. Na die voorlopige sintese is elektroniese stroombane ontwikkel om die aankomstyd van pulse vanaf die proporsionele neutronmonitortellingbuise saam met omgewingsveranderlikes soos temperatuur, druk en plek te bepaal, wat almal die tellingkoers beïnvloed.

Die MNM-DAS is suksesvol ontwerp en ontwikkel deur hierdie Stelselsingeneiursbenadering te volg wat ingebed is in ‘n ontwerpwetenskap navorsingsraamwerk. Dit word tans gebruik om neutrontellingsdata te voorsien in werklike-wêreld toepassings op internasionale vlak.

Sleutelwoorde: Neutronmonitor, ontwerpsnavorsing, kalibrasiemonitor

LIST OF ABBREVIATIONS

ADM	Advanced development model
CAD	Computer-aided design
CSR	Centre for Space Research
DSR	Design Science Research
EDM	Engineering development model
EMC	Electromagnetic conductivity
EMI	Electromagnetic interference
F/U	Functional unit
GPS	Global positioning system
HMI	Human machine interface
I/F	Interface
MCU	Micro-control unit
MNM-DAS	Mini-neutron monitor data acquisition system
NM	Neutron monitor
NMDB	Neutron monitor database
NTP	Network timing protocol
PCB	Printed circuit board
PPP	Pre-production prototyping
SANAE	South African National Antarctic Expedition
UART	Universal asynchronous receiver/transmitter
USB	Universal serial bus
XDM	Exploratory development model

TABLE OF CONTENTS

CHAPTER 1: INTRODUCTION

1.1 INTRODUCTION

Neutron monitors (NM) have been observing cosmic-ray activity since 1951 when J.A Simpson installed the first one at the University of Chicago [**1**]. The Centre for Space Research (CSR) of North-West University followed in 1957 and has now been involved with these types of observation for over 50 years. The CSR plays an important role in ground-based cosmic-ray research as it oversees a number of neutron monitors in the southern hemisphere. It operates four stations which span over 5000 kilometres from Antarctica to Namibia. This provides data at various latitudes which is important as the propagation of cosmic rays is influenced by the time-varying heliospheric magnetic field embedded in the solar wind, and by the geomagnetic field [**2**]. More detail on how these neutron monitors detect cosmic-ray activity is given in Chapter 2.

Despite the fact that neutron monitoring is a relatively old science, no standardisation has been achieved. All the monitors around the world make use of different proportional counters tubes and different electronic recording systems and this leads to significant differences in counting rates as argued in [**3**]. It is these differences that created the need for all the monitors to be calibrated against each other to enable comparison amongst all data sets. A team of scientists and engineers at the CSR designed and built such a calibration neutron monitor in 2003 [**4**] [**2**] [**5**]. This calibration demonstrated the functionality of a generation of CSR neutron monitors, and was used as an exploratory development model (XDM) in this research.

Developments in technology since 2003 necessitated the re-evaluation of this calibration monitor, and the CSR explored possible improvements and/or the redesign of the system. These researchers further saw the possibility that the new design could be used for more than just calibration standardization - it could also function as a recording system in its own right, with the potential to create a world standard for neutron monitors.

1.1.1 System layout

A neutron monitor consists of three critical parts. The extent and importance of each part may vary between monitors but in practical terms they are similar.

1. The counter tube: The standard tubes are filled either with $^{10}BF_3$ or ^{3}He, because ^{10}B and ^{3}He have a high cross-section for neutron capture. They vary in price and output capability, but essentially perform the same task. Multiple tubes can be used in parallel to gain more statistically accurate readings and cover more surface area, depending on the user requirements.
2. An electronic registration system: This includes a pre-amplifier and discriminator. The pulses generated by the counter tube need to be amplified sufficiently to distinguish it from noise by a discriminator
3. A data recording and storage unit. This is some form of recording system to enable the user to save the data.

A standard NM64 neutron monitor consisting of three $^{10}BF_3$ tubes, is shown in Figure 1-1.

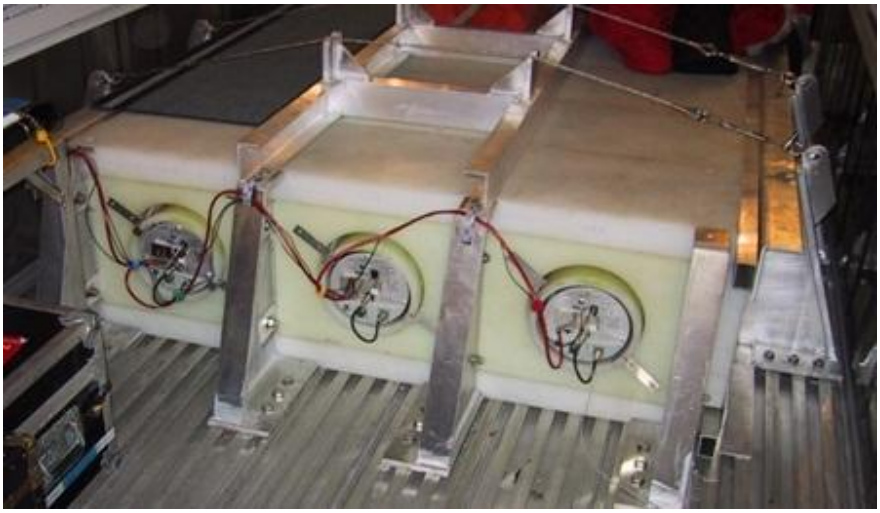

Figure 1-1: NM64 neutron monitor showing the tubes and amplifier

The calibration neutron monitor developed by the CSR in 2003 is shown in Figure 1-2.

Figure 1-2: Calibration neutron monitor system developed by the CSR in 2003 [2]

1.2 PURPOSE OF THE RESEARCH

An electronic recording sub-system is needed to serve as a replacement for the current calibration neutron monitor, which must yet be versatile enough to be adapted and used in the existing CSR neutron monitors. The purpose of the research was to design and develop such a sub-system.

From this point onward, the replacement for the calibration monitor will be referred to as the mini-neutron monitor (MNM) and the registration part of this system will be referred to as the mini-neutron monitor data acquisition system (MNM-DAS).

1.3 PURPOSE OF THIS STUDY AND RESEARCH METHODOLOGY

The development of a mini neutron monitor can be separated into two distinct parts, namely (i) the physical hardware and (ii) the MNM-DAS. This dissertation covers only the development of the MNM-DAS as the physical body of the neutron monitor will be largely the same as used for the calibration neutron monitor developed by the CSR in 2003.

The MNM-DAS was developed using Design Science Research (DSR) in conjunction with Systems Engineering (SE). The project workflow is shown in Figure 1-3. The project began with the proper formulation of the research question, along with the analysis of existing systems and identification of shortfalls.

A system architecture was drawn up in the conceptual design phase of the project (refer to Chapter 3 for more detail). This system architecture provided a coherent description of the essential system functions. An analysis of this conceptual design in the form of a resource allocation table showed the influence of failure of these functional units.

From the conceptual design and system architecture, a preliminary synthesis could be done. Following the preliminary synthesis, electronic circuitry was developed to capture the arrival time of pulses from the proportional neutron monitor counter tubes along with environmental variables, such as temperature, pressure, and location which all influence the count rate. The rigidity spectra of cosmic-rays also depend on geomagnetic coordinates; these can be derived from the GPS location, which is also logged. Rigidity spectra of cosmic-rays will be discussed in Section 2.1.1

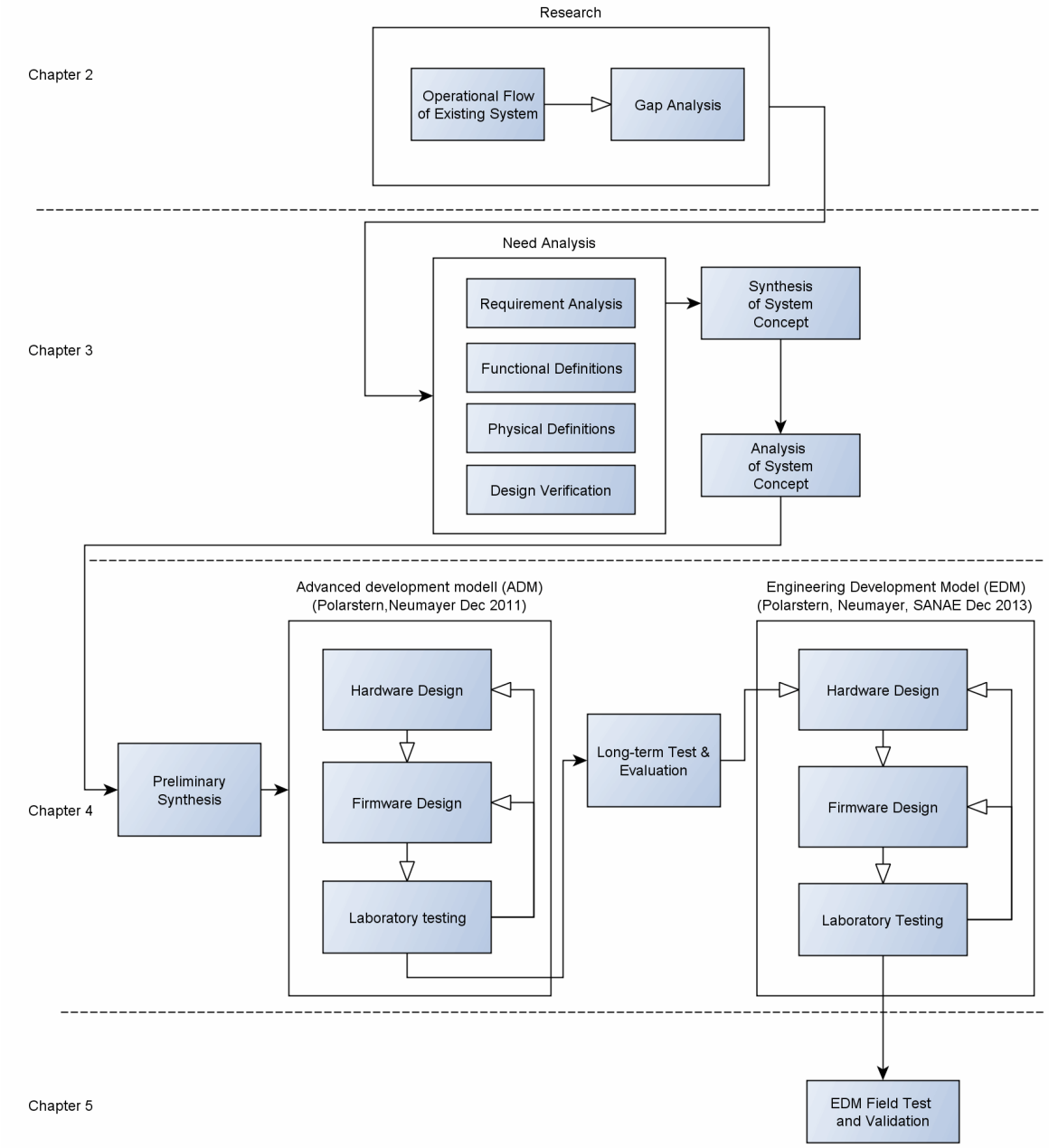

Figure 1-3: Project scope workflow

Each functional unit in the preliminary synthesis was developed and tested in an iterative process. The process of this method is discussed in detail in Chapter 2. The first iteration of the design process yielded the Advanced Development Model (ADM) which was implemented in December 2011 on the German science vessel, the Polarstern, and further

at the German Antarctic base Neumayer III in January 2012. The long-term testing continued for 14 months. In parallel with these tests, the system was optimized and additional features were added which yielded the Engineering Development Model (EDM).

Firmware was designed, programmed and implemented on the system's micro-controllers. The firmware was designed in such a way that it can perform self-diagnostics and self-repair where possible. The MNM-DAS connects to an on-site file transfer protocol (FTP) server where neutron count data is stored. USB flash storage is used as backup for the important neutron count data.

Finally, the system was tested and verified as a complete unit by referring to the functional requirements as defined in user requirements. Data that had been generated was analysed to ensure that the system provided all required functional capability and performance requirements. The ADM was replaced by the EDM on the Polarstern; and at Neumayer III at the end of 2013.

The verification of the system was done through a series of experiments discussed in Chapter 5. Verification and validation of the data is provided and discussed in Chapters 5 and 6.

1.4 OVERVIEW OF STUDY

The introduction to cosmic-ray detection is provided in Chapter 1, followed by the concept and guidelines of Design Science Research (DSR). These guidelines were followed during the design of the MNM-DAS.

Chapter 2 contains a literature study, where an overview of the calibration monitor system is provided, together with the objectives for the development of the MNM system. The shortfalls of the calibration monitor are discussed, as well as possible new additions. This Chapter further deals with the method of combining DSR and SE to synthesise the MNM-DAS.

The conceptual synthesis of the MNM-DAS is provided in Chapter 3. This chapter focuses on the system architecture. This architecture will show not only the functions that have to be performed, but also how they will be integrated to form the MNM-DAS.

Chapter 4 describes the detailed synthesis phase. This chapter also serves as a detailed design description and contains sufficient detail to describe the MNM-DAS development model. The firmware and software designs are shown in state diagrams and subsequently discussed.

Chapter 5 describes empirical testing and verification of the system. This is done by using data obtained from laboratory testing, as well as implementation results on the Polarstern and Neumayer III. The verification data of the system is given in graphic format.

Finally, in Chapter 6, conclusions are drawn on the integration and implementation of DSR and systems-engineering, that had been used to develop a MNM-DAS; proposals for future work and possible improvements are presented.

CHAPTER 2: LITERATURE STUDY: NEUTRON MONITORS AND DESIGN SCIENCE RESEARCH PHILOSOPY

This chapter provides background on the neutron monitor project at the CSR and provides substantiation as to why an MNM-DAS was required. This chapter also provides information on how neutron monitors function and gives an introduction to existing systems, as well as a discussion of the shortfalls and possible room for improvement. It further explains the objectives of the new system and deals with the design philosophy that was followed to achieve these objectives.

2.1 NEUTRON MONITORS

2.1.1 Programme background

Neutron monitors detect secondary particles produced by the collision of cosmic rays and atmospheric nuclei. These cosmic rays are high-energy particles travelling through space with energies greater than 1 GeV. The first neutron monitor (the Climax NM) was installed in 1951 by J.A Simpson of the University of Chicago [**1**], [**2**], [**6**]. In 1957/8 Simpson extended the monitor to a 12-counter neutron monitor (called the IGY) which was deployed in a worldwide network during the International Geophysical Year. Shortly afterwards the NM64 super neutron monitor was designed by H. Carmichael for deployment in time for the International Quiet Sun Year (1964). Using unusually large $^{10}BF_3$ proportional counters made at Chalk River, Canada, Hatton and Carmichael in 1964 comprehensively studied the experimental design of the NM64. Consequently the efficiency of neutron counters in recording evaporation neutrons produced in the lead of a monitor increased from 1.9% for the IGY to 5.7% for the NM64, an increase of 3.3 times the counting rate per unit area of lead producer [**7**]. This is an important enhancement as higher counting rates produce greater statistical accuracy.

Neutron monitors proliferated to a network of more than one hundred by the end of the 1960s. At present there are still approximately 50 neutron monitors in operation [**2**]. The CSR at the North-West University operates four of these monitors, three NM64s at SANAE IV base, Tsumeb and Hermanus and one IGY at Potchefstroom. They span over 5000 kilometres, from Antarctica to Namibia [**8**]. This network provides data at various latitudes, which is important as the propagation of these particles is influenced by the geomagnetic field. This is more accurately expressed in terms of rigidity, which is the energy per charge required to penetrate the geomagnetic field. To penetrate through this geomagnetic field, the particles must have a rigidity that exceeds the geomagnetic cut-off rigidity for a given position. Cut-off rigidities around the world can be seen in Figure 2-1.

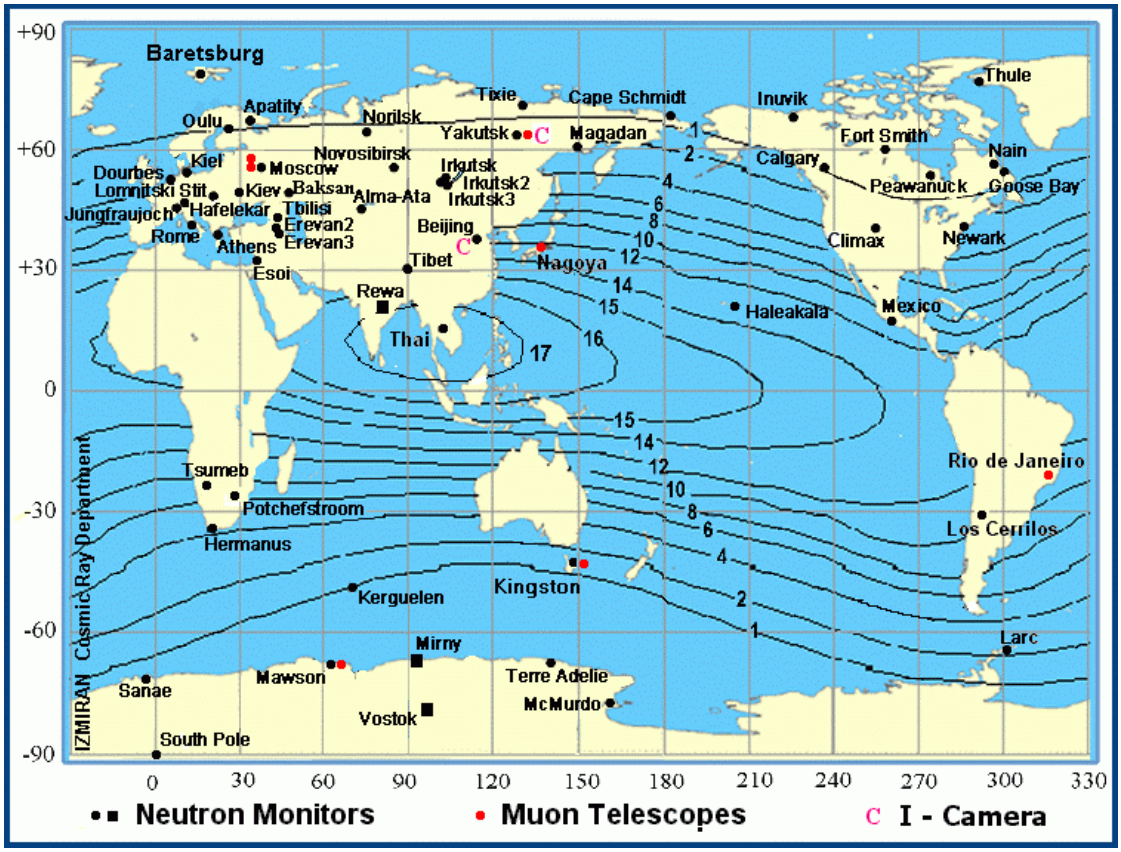

Figure 2-1: Illustration of the effective vertical cut-off rigidities for a world grid [2] most of the currently operating neutron monitors are also shown

In short this means that neutron monitors placed at the poles can detect particles with rigidities higher than 1 GV while they can detect only particles with rigidities higher than 15 GV near the equator.

The normalized counting rate for these stations operated by the CSR is shown in Figure 2-2 along with their cut-off rigidities. An inverse 11-year solar cycle can clearly be seen by looking at the counting rates, with the highest amplitude at SANAE IV which has the lowest cut-off rigidity [**2**]. This inverse correlation between solar activity and the amount of cosmic rays detected is due to the sweeping effect of the sun.

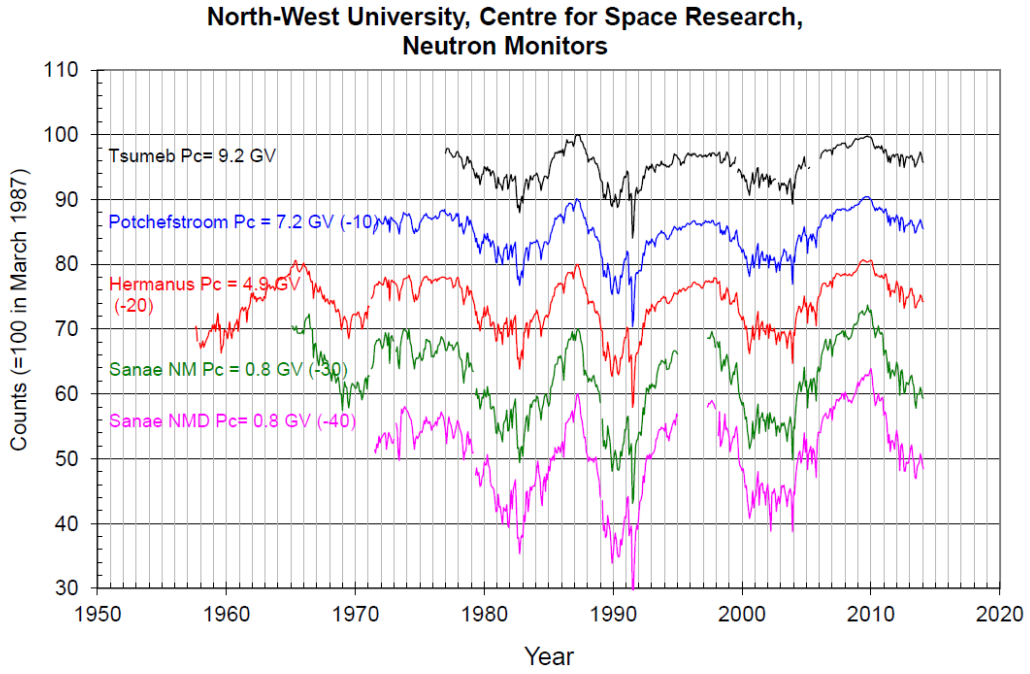

Figure 2-2: Monthly-normalised counting rate of the four neutron monitors at SANAE, Hermanus, Potchefstroom and Tsumeb respectively [23**].**

The spectra of cosmic-rays can be derived, in principle, from the difference in counting rates of neutron monitors at different cut-off rigidities around the world. However, in practice, this is not possible because the efficiency of each monitor differs and thus the counting rates cannot be compared. Therefore, to investigate the energy dependence of the

modulation of cosmic rays, it is required that the counting rates must be normalised sufficiently accurately against one another to within about 0.2% [**4**].

Towards the end of the 20th century the need for worldwide inter-calibration of these large, stationary neutron monitors was realised, which resulted in the design and construction of two calibration neutron monitors at the Potchefstroom Campus of the North-West University [**9**].

Alongside the need for calibration, there was also a need for the creation of an international data pool of all these neutron monitors. This system, now in its developmental stages, is called the neutron monitor database (NMDB) [**10**]. Together, these two resources will make it possible to calculate the full spectra of events.

It is with this project that the North-West University foresaw that should these calibration monitors, developed in 2003, be able to be used as neutron monitors in their own right it would open up further opportunities of research. The reason for this will become evident soon.

Ground-based detectors such as NMs do not record cosmic rays directly. On the final step of their journey cosmic rays penetrate the atmosphere, causing reactions with nuclei of air molecules. This reaction produces secondary particles (neutrons, protons, mesons, electrons and photons) as illustrated in Figure 2-3. A NM is sensitive to the neutron component of these secondary particle showers.

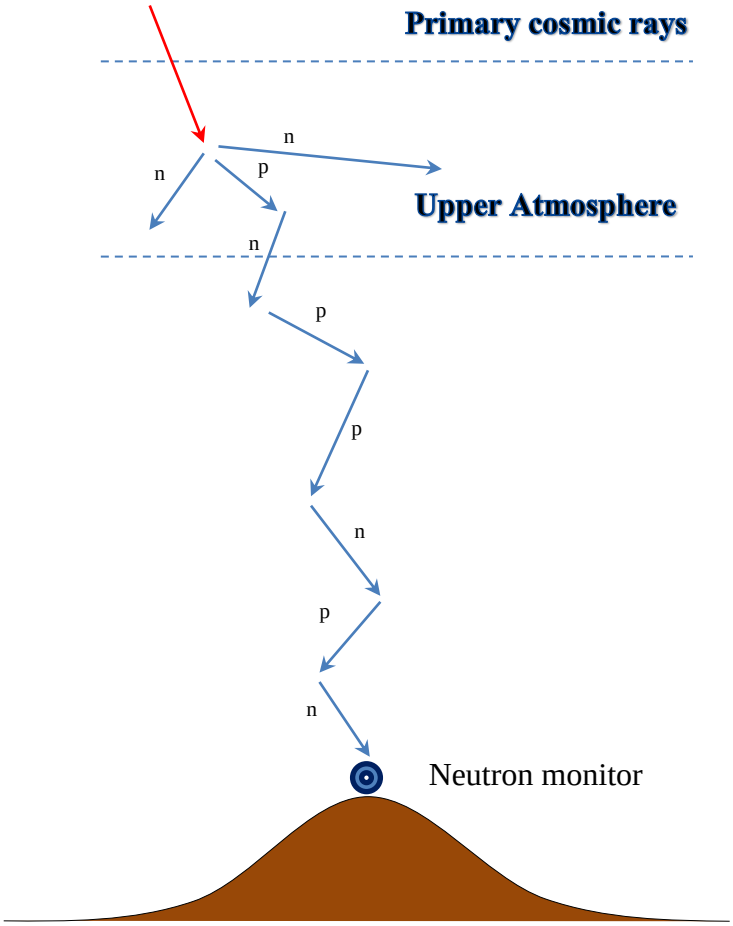

Figure 2-3: Scattering shower of a cosmic ray

The shower of secondary particles reaches its maximum extent in the top 10 % to 20 % of the atmosphere, i.e. between 100 mbar and 200 mbar. Thereafter the shower decays exponentially according to

$$\frac{dN}{N} = -\beta\, dP \qquad \textbf{(Eq 2-1)}$$

where dN = change in the counting rate N,

β = barometric coefficient, and

dP = change of the atmospheric pressure.

This expression can be integrated to yield

$$N = N_0 e^{\beta(P_o - P)} \qquad \textbf{(Eq 2-2)}$$

where N_0 = the counting rate at a reference pressure P_0.
The barometric coefficient has a typical value of -0.007 mbar^{-1}.

The barometric equation for atmospheric pressure is

$$P = P_0 e^{\frac{-mg}{kT}} \quad \textbf{(Eq 2-3)}$$

where m is mass of air particles (80 % Ne; 20 % O_2),
T is atom temperature,
g is gravitational acceleration, and
k is the Boltzmann constant.

For a temperature of 20 °C (293.15 K), the constants are such that

$$P \approx P_0 e^{-0.00012h} \quad \textbf{(Eq 2-4)}$$

with h measured in meters above sea level.

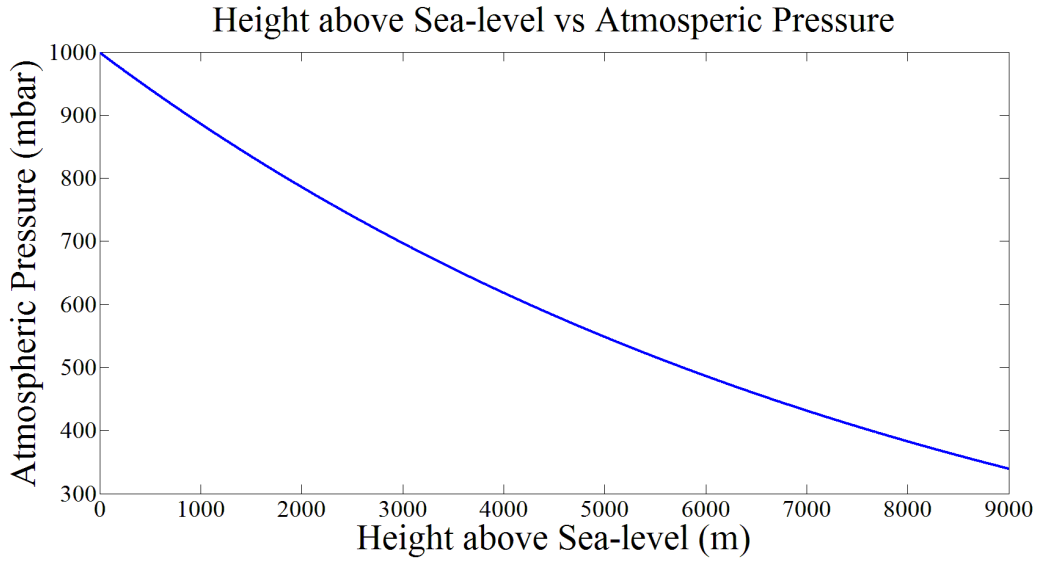

Figure 2-4: Equation 2-2. Height above sea-level vs atmospheric pressure

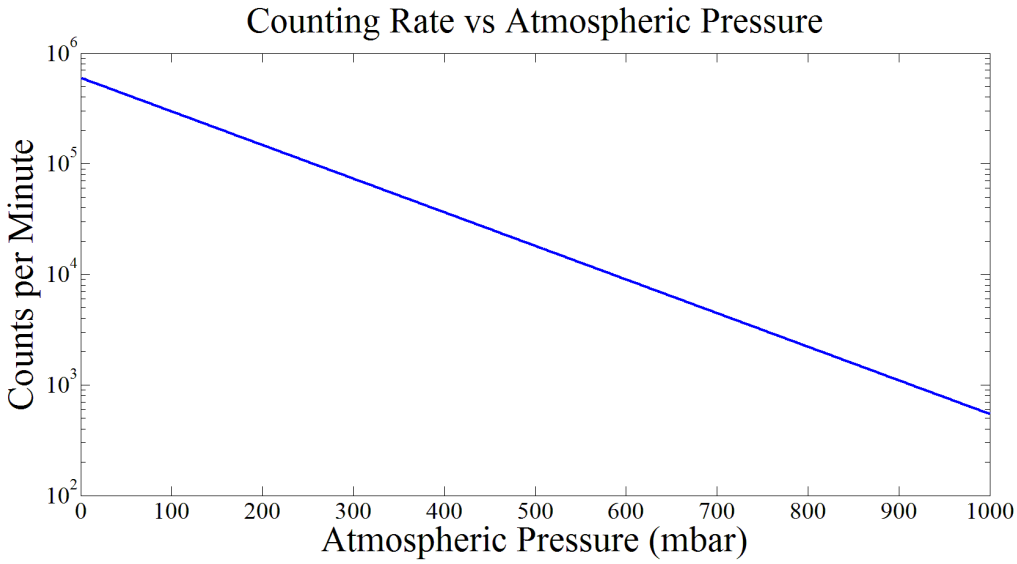

Figure 2-5: Equation 2-3. Counts per minute vs atmospheric pressure

Figure 2-4 and Figure 2-5 depict Equations (2-4) and (2-2) and show that higher altitude provides lower atmospheric pressure, and lower atmospheric pressure provides higher counting rates. This, in turn, will provide higher statistical accuracy.

The larger the neutron monitor, the more surface area is covered and the higher the counting rate. However, a larger size implies an increase in weight and cost. Therefore, the idea behind the mini-neutron monitor is that it is mobile enough to be transported to higher altitudes at less cost. Its counts will be lower due to the smaller size but due to the increase in altitude, as explained in this section, the counts will also increase. For instance, if a neutron monitor is placed at 3200 m above sea level, the atmospheric pressure will be about 680 mbar, which in turn will yield a counting rate nine times higher than at sea level. This method will make the entire system less expensive and yet remain as effective.

A Finnish group ordered two MNM to be placed at Dome C at an altitude of 3200 m. The German research station (Neumayer III) and research vessel (Polarstern) have already installed the design at sea level. They prefer this design because of the relatively low cost and the minimal space requirements. The most recent installation is in Mexico and has been placed at an altitude of 4200 m (giving sixteen times the counting rate than at sea level).

2.1.2 Physics behind cosmic-ray detection

Detectors for slow and thermal neutrons are based on the (n,p) and (n,α) reactions. The isotope ^{10}B is commonly used by an ionisation chamber or a proportional counter filled with $^{10}BF_3$ gas. The exothermic reaction is given by

$$^{10}\mathrm{B} + n \Rightarrow {}^{7}\mathrm{Li} + {}^{4}\mathrm{He} + 2.78 \ \mathrm{MeV}\ (6\%) \qquad \textbf{(Eq 2-5)}$$

$$^{3}\mathrm{He} + n \Rightarrow {}^{3}\mathrm{H} + p + 0.765 \ \mathrm{MeV} \qquad \textbf{(Eq 2-6)}$$

^3He naturally exists in gas form; to get ^{10}B in gas form it has to be in the form of $^{10}BF_3$, which is extremely toxic. Thus it is preferred to use ^3He; however, it is extremely expensive and, therefore most NMs work with $^{10}BF_3$, as with the MNM.

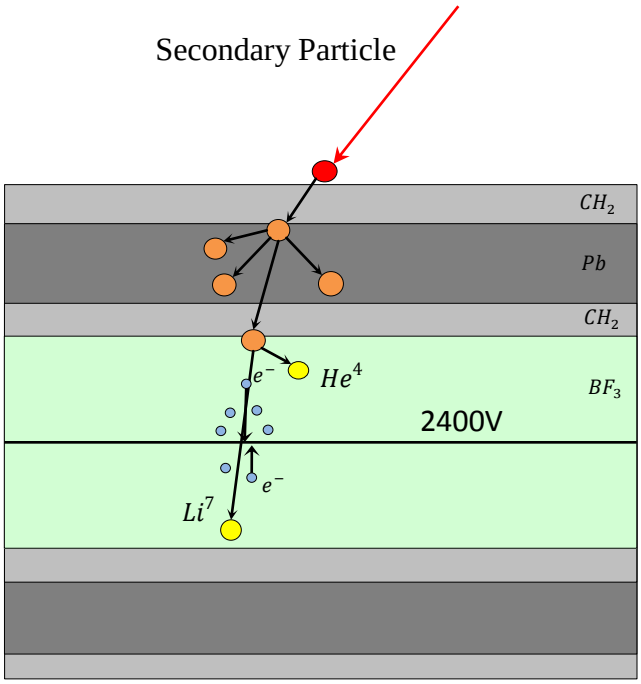

Figure 2-6: Particle reaction inside a gas-filled detector

A $^{10}BF_3$ counter tube is a cylinder filled with $^{10}BF_3$, and at the centre of this cylinder is an extremely thin wire that is kept at high voltage. This creates an outwardly directed electrical field inside that tube with

$$E \propto \frac{1}{r} \quad \textbf{(Eq 2-7)}$$

Where r is the radial distance from the centre wire and E is the Electric field.

The $^{10}BF_3$ tube operates in the proportional region where the electric field is so strong in a certain fraction of the counter volume that the electrons from the primary ionization acquire enough energy between collisions to produce additional ionizations. This amplification effect is called gas amplification and it creates a cloud of electrons on the wire which can produce a charge of up to 10^{-12} C. In the proportional region the number of electrons produced is fairly independent of the high-voltage Figure 2-7 shows this region of operation (Plateau region).

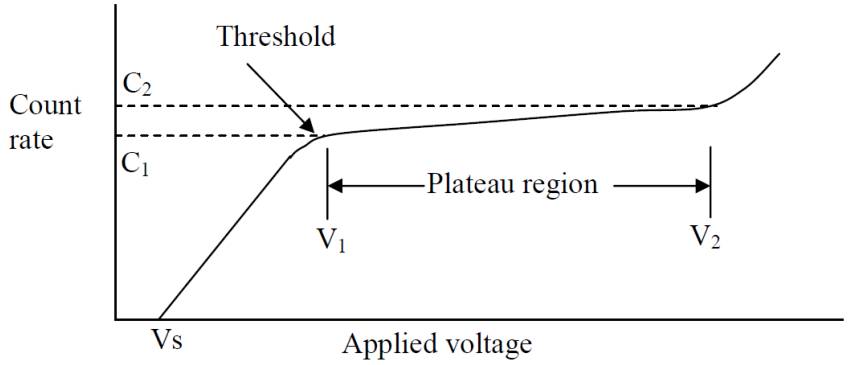

Figure 2-7: Characteristics of a gas-filled detector [11]

The reaction of Eq 2-5 is only effective if the neutrons are thermal. To slow down the neutrons that cause the reaction in Eq 2-5, the counter tube is placed inside a moderator. Even then, only one in ten of these incoming neutrons causes a reaction in the counter tube. To increase this, a lead ring is placed around the moderator which produces about ten secondary neutrons for every neutron that enters. This is called the multiplication effect. A

reflector is placed around the multiplier in an attempt to keep the neutrons produced inside, so that they can be registered. The reflector also serves as a shield to keep atmospheric neutrons out [**11**].

2.2 OVERVIEW OF THE EXISTING CALIBRATION NEUTRON MONITOR

This section deals with the existing calibration monitor. A photograph of this calibration monitor can be seen in Figure 1-2 page 3.

2.2.1 Analysis of the calibration neutron monitor

The architecture of the existing system as seen in Figure 2-8 was derived from the physical calibration monitor shown in Figure 1-2 on page 3.

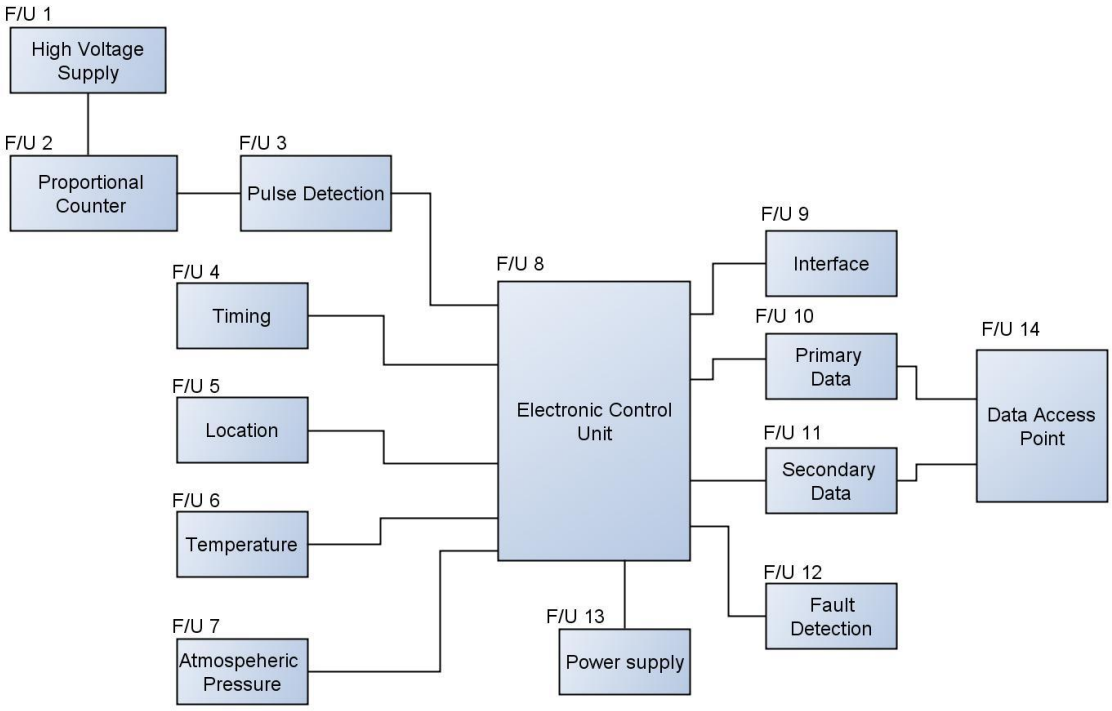

Figure 2-8: Architecture of existing system

F/U 1 provides the ^{3}He tube (F/U 2) with 1470 V to operate in the correct gas amplification region as discussed in the previous section. F/U 3 uses a pre-amplifier to amplify detected pulses sufficiently to be discriminated by a discriminator. The discriminator is a pulse height detector which provides a 5 V output pulse if the input increases over a predetermined voltage and is implemented in F/U 8. All pulses below this predetermined voltage are assumed to be noise.

A GPS module, F/U 4 & 5, provides the embedded PC, F/U 8, with an accurate time reference as neutron monitors need to be synchronised to UTC time to facilitate data comparison between stations. The GPS module also provides the embedded PC with location information in order to calculate cut-off rigidity.

All data processing, storage, and distribution are done by the embedded PC, FU 8. The discriminator output is connected via serial ports and data recorded on a per-second basis. The two environmental variables that can affect neutron monitor detection are also recorded with a pressure sensor (F/U 6) and a temperature sensor (F/U 7).

Data is stored on a hard drive, F/U 10, and mirrored on an identical hard drive, F/U 11, for backup purposes. The primary method of data retrieval is by unplugging one of the hard drives and downloading the data to whichever data point, F/U 14, is required.

The HMI, F/U 9, consists of an LCD screen, LED indications and a keypad. Fault detection is done in code on the embedded PC.

2.2.2 Shortfalls of the existing system

This section describes the most important shortfalls of the 2003 calibration monitor, should it be used as a neutron monitor.

2.2.2.1 Physical size

The existing system is too large (see Figure 1-2) to use in a NM64 neutron monitor, as the dimensions of the recording system are more than double the available space. The size also

provides a logistical problem as it is difficult to transport larger objects safely, especially to remote destinations such as Antarctica.

2.2.2.2 Storage method

The current calibration monitor makes use of a hard-drive mirroring system operated from a built-in PC. There is thus no off-site redundancy or data backup system in the event of failure.

2.2.2.3 Modularity

Repairs of these types of systems in the field are extremely difficult; hence, a system is required that has sufficient modularity to replace only faulty modules. Field repairs are almost impossible as the entire system needs to be taken to an equipped laboratory for repair and testing.

2.2.2.4 Documentation

The biggest shortfall of the system is the lack of a properly documented physical configuration. Though some documentation exists, it is not sufficient to reproduce this system. There is sufficient information with which to repair the system, but without proper documentation the system cannot be reproduced, which is a major shortfall.

2.2.2.5 Fault detection

The current calibration monitors require on-site personnel for daily checks to handle fault detection. This is tedious and cumbersome and has the potential to lead to longer intervals between checks, which in turn may cause prolonged downtime, should an error occur.

2.3 OBJECTIVES OF A MNM-DAS

The primary objectives of the NMN-DAS developed in this work are listed below:

- Provide a method for proportionally counting cosmic rays;

- Record environmental variables such as location, temperature and pressure;
- Replace the registration system of the calibration monitor, and;
- Eventually replace the registration systems of the NM64 of the CSR at SANAE, Hermanus, Potchefstroom and Tsumeb.

2.4 DESIGN PHILOSOPHY

This research utilized a combination of systems engineering for development and design science research as a research philosophy. The following section deals with the combined systems engineering and DSR method with subsequent chapters referring back to this section to show that a process was followed corresponding to the methodology discussed in this chapter.

2.4.1 Design science research

Sections 2.4.1.1 to 2.4.1.3 give a summary of Alan R Hevner's work published in 2004 [**12**] [**13**]. His article [**12**] was the seminal article for design science research. Additions to his work are discussed in Section 2.4.1.4 and thereafter.

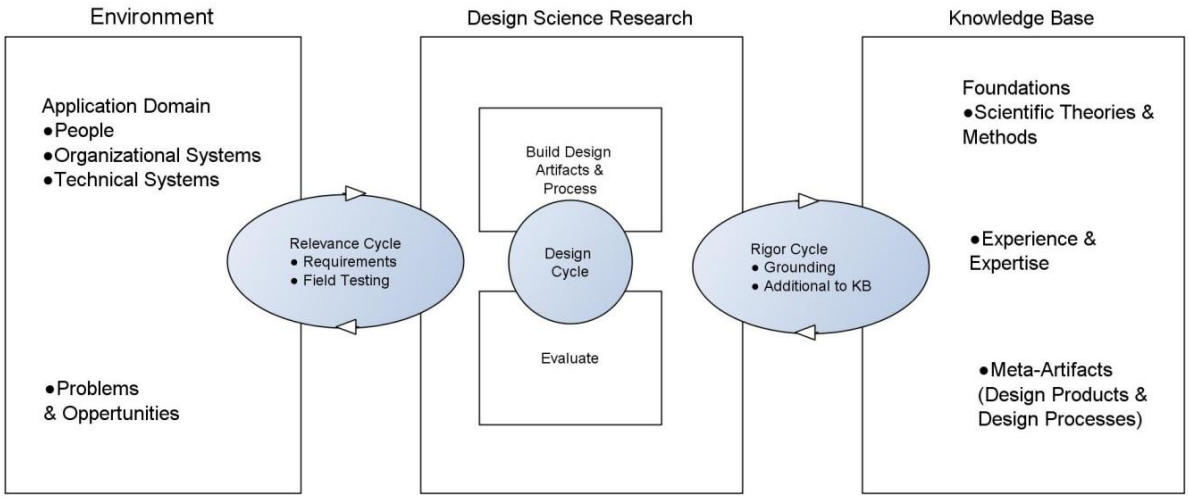

Figure 2-9: Design science research life cycle adapted from [12**]**

DSR has three cycles in a design science research project as shown in Figure 2-9

Figure 2-9: Design science research life cycle adapted from

, as adapted from [**12**].

The Relevance Cycle bridges the contextual environment of the research project with design-science activities. The Rigor Cycle connects the design-science activities with the knowledge-base of scientific foundations, experience, and expertise that informs the research project. The central Design Cycle establishes iterations between the two core activities of building and evaluating the design artefacts and the processes of research. The three cycles above must be present and clearly identifiable in a DSR project. The following sections briefly expand on the meaning of each cycle.

2.4.1.1 Relevance cycle

> *Design science research is motivated by the desire to improve the environment by the introduction of new and innovative artifacts and the processes for building these artifacts* [**14**] page 17.

In this case it will be the design of the MNM-DAS and the method used to synthesise this artefact. DSR begins with the identification of a need in the application environment. A needs analysis provides not only the requirements for the artefact but also the acceptance criteria for validation of the artefact. The output from the DSR must thus be returned to the environment for study and evaluation in the application domain. The results of field testing in the application domain will then determine whether additional iterations of the relevance cycle are required. Should the field test show deficiencies in functionality or in the inherent qualities of the artefact, additional cycles will be required until the validation of the artefact has been proven.

2.4.1.2 Rigor cycle

Design science draws from a vast knowledge base of scientific theories and engineering methods that provides the foundation for DSR. The knowledge base contains two types of knowledge:

- The experiences and expertise that define the "state of the art" in the application domain of the research; and
- The existing artefacts and processes found in the application domain.

As an example in the case of the MNM-DAS, experiences and expertise were used to create an abstract architecture of the existing calibration monitor. This added to the knowledge base to be drawn upon in future research and development.

The use of knowledge from existing systems and artefacts ensures that the design is a valid research and development contribution and not a routine design based on known applications and design processes. It is important to thoroughly research and reference the past knowledge base to ensure improvement.

Consideration of rigor in the design research is based on the researcher's skilled selection and application of appropriate theories and methods for constructing and evaluating the artefact. DSR is grounded on the existing ideas drawn from the knowledge base.

Additions to the knowledge base as result of design research include any additions of extensions to the original theories and methods made during the research, and all experiences gained from performing the iterative design cycles and field testing in the application domain [**12**].

2.4.1.3 Design cycle

The internal design cycle is the core of a DSR project. This cycle of research activities iterates rapidly between the construction of an artefact, its evaluation, and subsequent feedback to refine the design. The nature of this cycle is to generate design alternatives and evaluate alternatives against requirements until a satisfactory design has been achieved [**12**].

It is important to understand the dependence of the design cycle on the other two cycles while appreciating its relative independence during the actual execution of the research. During the performance of the design cycle, a balance must be maintained between the

efforts spent in constructing and those spent evaluating the evolving design artefact. Both activities must be convincingly based on relevance and rigor [**12**].

Having a strongly grounded argument for the construction of the artefact, as discussed above, is insufficient if the subsequent evaluation is weak. Artefacts must be rigorously and thoroughly scientifically tested before being released for field testing in the relevance cycle. Failure to do so can have serious time and financial consequences. This calls for multiple iterations of the design cycle before contributions are reintroduced into the relevance and rigor cycles [**12**].

2.4.2 Embedment of systems engineering in DSR

Figure 2-10 on the following page shows how systems engineering is incorporated into the DSR process. It uses the broad methodology of DSR, but replaces the internal design cycle with a systems-engineering approach to minimize the design cycles and to maximize the quality of the research output. It also adds structure to the design cycle to give direction to the design and verification process.

Once the need has been identified in the real-world environment, it must be analysed. This validates the need and requirements that must be met. From this needs analysis, a conceptual design must be created to show that the conceptual solution is valid and that the concept addresses all requirements set out in the need analysis. This is done using a resource allocation table that shows all requirements of all sub-systems to be used as input to the detailed design phase. After each phase, the results from a phase are evaluated and added to the knowledge base. This differs slightly for normal DSR as the rigor cycle in the combined SE / DSR method is more intense and the addition of the knowledge base more frequent and controlled.

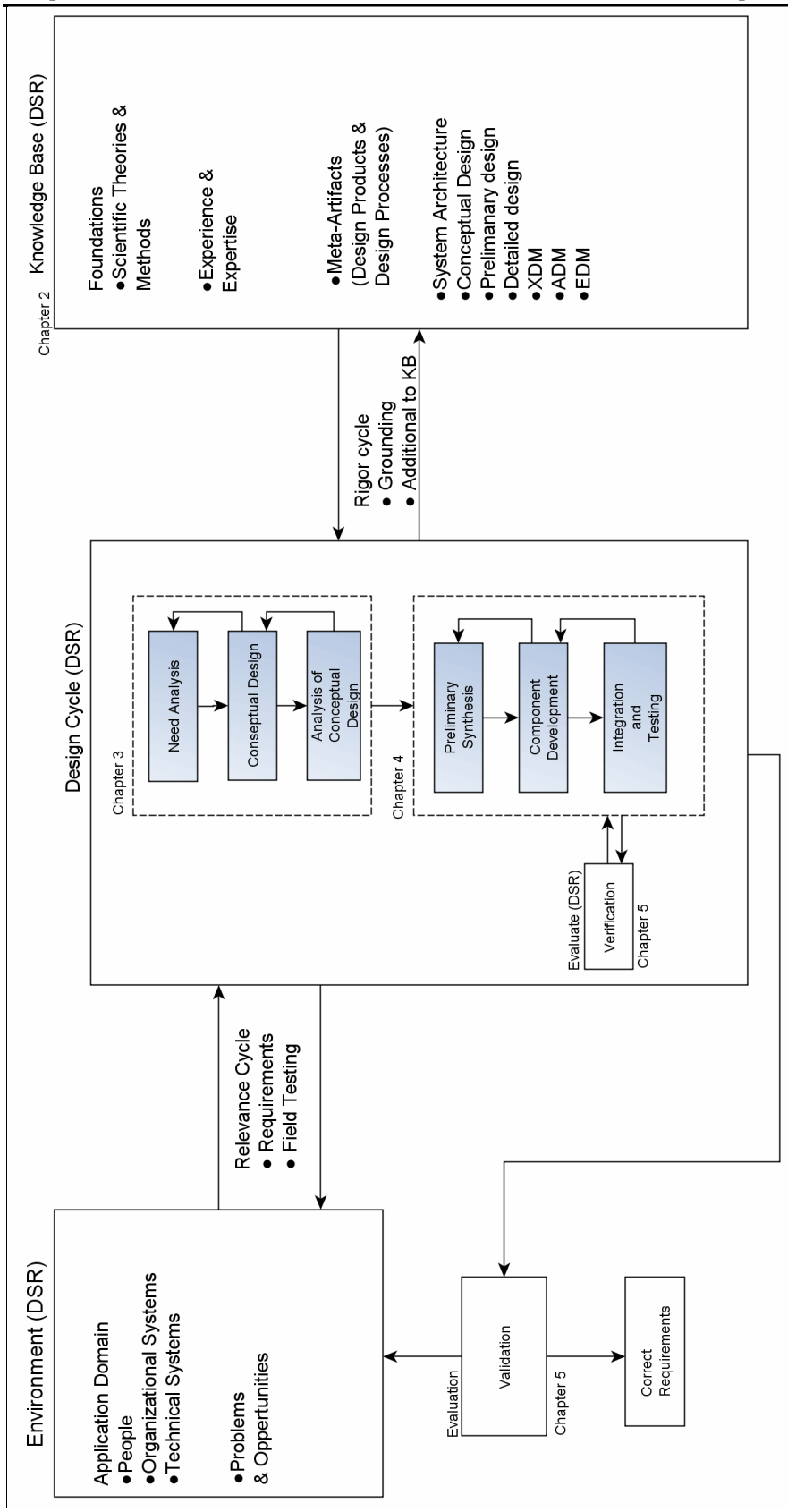

Figure 2-10: Encapsulation of systems engineering in DSR

Once the detailed design has been concluded, sub-systems are thoroughly tested and are integrated and tested as a unified system. Testing and evaluation constitute an on-going process. After successful integration and testing in the laboratory setup, the resulting physical system is introduced to the external environment (real world) for final testing and evaluation, which is in essence the validation of the system.

2.4.2.1 Conceptual design

The conceptual design is described in Chapter 3, and broken down even further as shown in Figure 2-11.

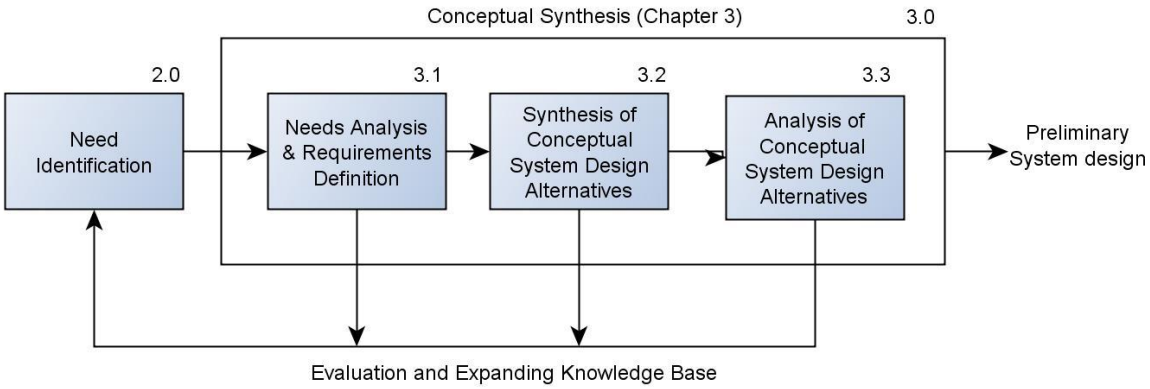

Figure 2-11: Conceptual systems engineering design process, adapted from [20**]**

2.4.2.1.1 Needs analysis

As discussed in Section 2.4.1, the need is identified in the application domain. This need will serve as input to the conceptual design phase. The objective of the needs analysis is best described by [**15**] on page 139.

> *The primary objective of the need analysis phase of the system life cycle is to show clearly and convincingly that a valid operational need (or potential market) exists for a new system or a major upgrade to an existing system, and that there is a feasible*

approach to fulfilling the need at an affordable cost and within an acceptable level of risk

There may be numerous requirements, such as system cost, size, weight, performance and a project time-frame to consider. The needs analysis will serve as validation criterion once the artefact has been introduced into the environment. With the iteration between the design phase and the environmental introduction, it is possible that requirements of the system may have to be adjusted. A system might meet current criteria but may be ineffective (or incapable) in terms of new criteria revealed in the environment during testing.

2.4.2.1.2 Synthesis of concept

After the needs analysis has been completed, a conceptual design must be performed. The conceptual design converts the operational requirements of the system into a concept definition that addresses all requirements. This provides a quantifiable basis for selecting an acceptable functional and physical system concept. This conceptual design is an early high-level life-cycle activity that has the potential to establish and commit the function, form, and fit of sub-systems.

In the case of the MNM-DAS, an objective of the conceptual design was to create an abstract system-architecture. This abstract architecture must remain valid as long as the operational objective set in the need analysis remains the same. This systems architecture forms part of the knowledge base and can be drawn upon in future iterations of the design phase.

2.4.2.1.3 Analysis of concept

The analysis of the concept is done with the help of a resource allocation table, or matrix. This resource allocation links functions to resources and provides a means to do failure-mode analysis. Each resource failure affects functions at different levels; these failures may be identified from a resource allocation table.

2.4.2.2 Detail design and development (Chapter 4)

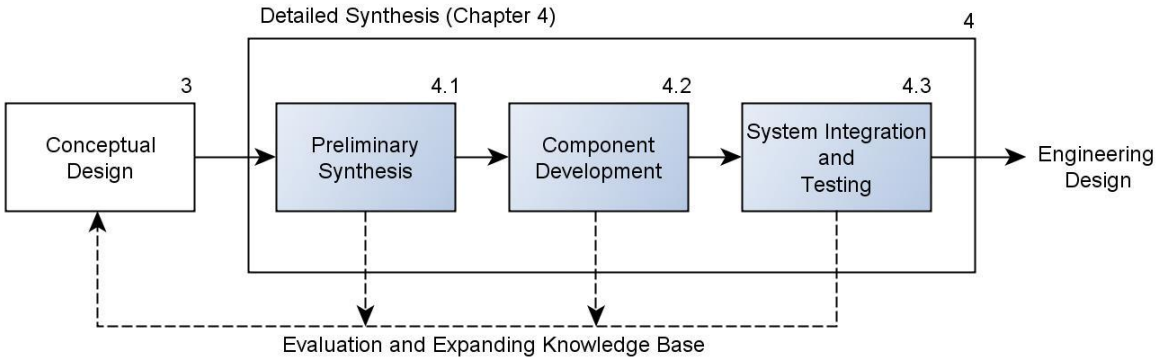

Figure 2-12: Conceptual systems engineering design process

The detailed design of the project is divided into three sections as shown in Figure 2-12.

2.4.2.2.1 Preliminary design

The preliminary design phase bridges the gap between the high level of the systems architecture and the low-level component development phase. It defines the functions and interfaces for each higher-level function at a lower level. The preliminary design includes the lower-level functional flow, functional architecture, and performance of the system.

2.4.2.2.2 Detailed design

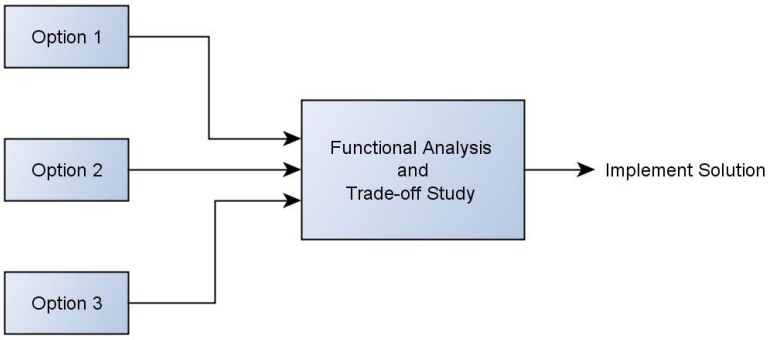

Figure 2-13: Advanced development process

The process of this development phase is shown in Figure 2-13. The objective of the detailed development phase is to implement the functional designs of the system elements as physical hardware and software components. This will define all components that make up the higher-level system definition. A trade-off analysis, in the form of multiple-criteria decision analysis (MCDM), is used to ensure that correct decisions are made with respect to component selection. This minimizes the required number of iterations of the development cycle and reduces development time and cost. All functional requirements and applicable constraints are taken into account when performing a trade-off analysis.

2.4.2.2.3 System integration and testing

Integration of lower-level functional units – such as physical electronic components, modules, and software – is achieved by using the higher-level architecture and interfaces. Interface definitions simplify integration, while functional and performance evaluation is done during component, module and system testing.

A proper test plan will take into account the functional capability of each component, module, and system. Performance testing will be simplified when test planning is done beforehand, where laboratory tests will verify the design in a controlled environment and field tests will validate the design in practice.

CAD modelling is vital to the structural integrity of the physical system. Knowing where and how each component will be mechanically positioned and secured is important for tool accessibility. Easily reachable fasteners can significantly reduce assembly time, especially if it is done manually. In addition, proper component placement can be done by using CAD modelling for thermal design.

When placing each component, electromagnetic interference must be taken into account; correct component EMC design will significantly reduce electromagnetic interference in an electronic system. In the design of a monitor, factors such as high-voltage effects must be considered as part of interference, such as creepage distances between high-voltage nodes and low potential copper paths.

To summarize, integration and testing are significantly simplified when all "design for" criteria and high level functional requirements have been defined and addressed early on in the design. This can be done effectively by using systems engineering principles embedded in a design science research approach, which significantly reduces research time and increases value by supplementing the knowledge base.

2.5 SUMMARY

This chapter provided an overview of the global relevance of the neutron monitor network and how neutron monitors function. It further highlighted the relevance of a calibration monitor and the benefits of utilizing such a monitor at high altitudes. It discussed the shortfalls of the calibration monitor developed in 2003 by the CSR as a monitor in its own right.

This chapter also discussed the design science research methodology and proposed a systems engineering approach embedded in DSR methodology to enhance the relevance of the research outcome and to streamline the design and verification processes. Using this hybrid approach, a high-level architecture was extracted (abstracted) from the existing physical implementation of the calibration monitor to describe the function and fit of all functional units that make up the calibration monitor.

The abstraction, background knowledge and adapted DSR methodology are applied in subsequent chapters to define lower-level functions and to provide a framework within which research can be effectively conducted.

CHAPTER 3: CONCEPTUAL SYNTHESIS AND EVALUATION

3.1 INTRODUCTION

This chapter deals with the conceptual design and evaluation of the MNM-DAS. Figure 3-1 shows the operational flow of the conceptual design process. The identified need served as input to this phase of the design. The synthesis process of the conceptual design was divided into three sections, as described in Sections 3.2 to 3.4. In Section 3.2 the need identified in the environment was further analysed to give tangible objectives through analysis. The result of this needs analysis was used as input to synthesise the concept in Section 3.3. As discussed in Chapter 2, the conceptual design was analysed by using a resource allocation table in Section 3.4.

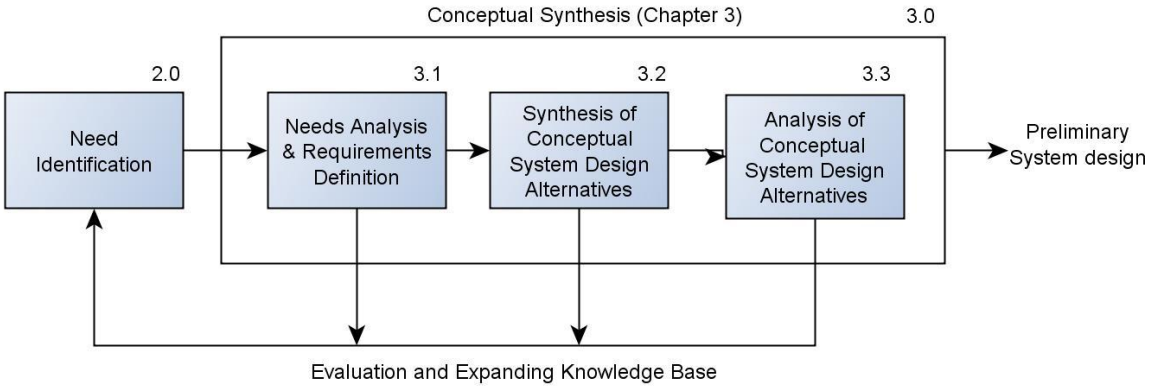

Figure 3-1: Conceptual system engineering design process [19]

The system requirements discussed in Sections 3.2 on page 31 serve as input to this functional unit. These are specific constraints to consider for this unit as seen in Figure 3-2.

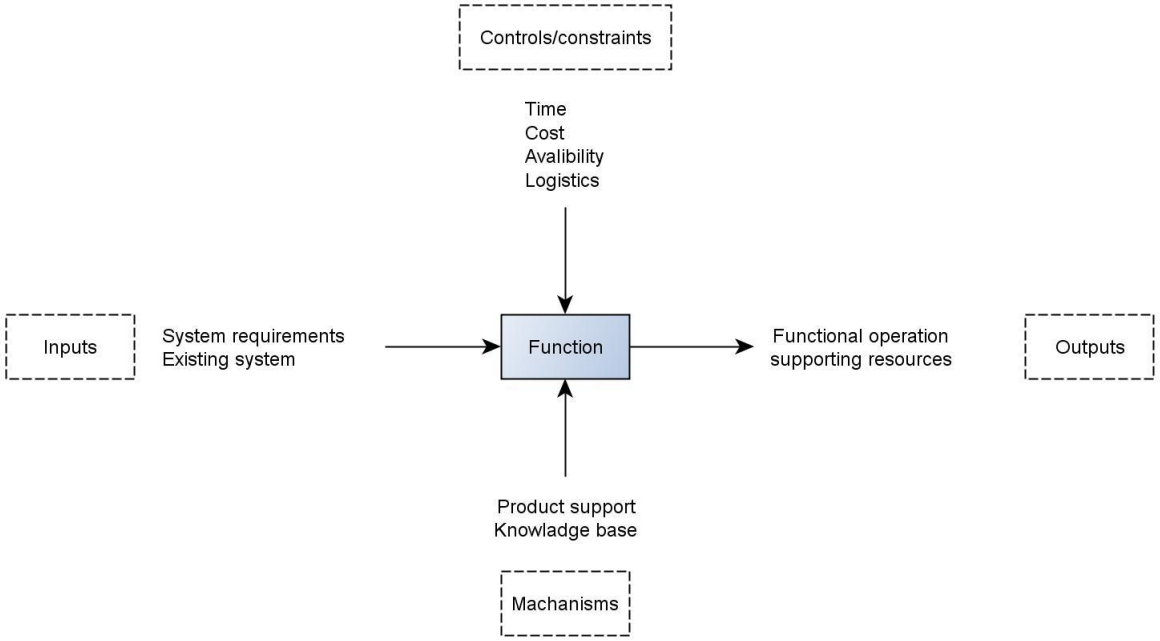

Figure 3-2: IDEF-0 diagram of conceptual design

3.2 REQUIREMENTS ANALYSIS

A high-level requirements analysis takes the need identified in the environment to a system comprising functions. This analysis serves as validation to ensure that the operational requirements, including high-level functional requirements, of the system can be referenced at every stage of the development process. The needs analysis divides requirements into four categories, namely operational-level functional requirements, (derived) lower-level functional requirements, performance requirements and constraints. This functional breakdown is shown in Figure 3-3 in the form of an objectives tree.

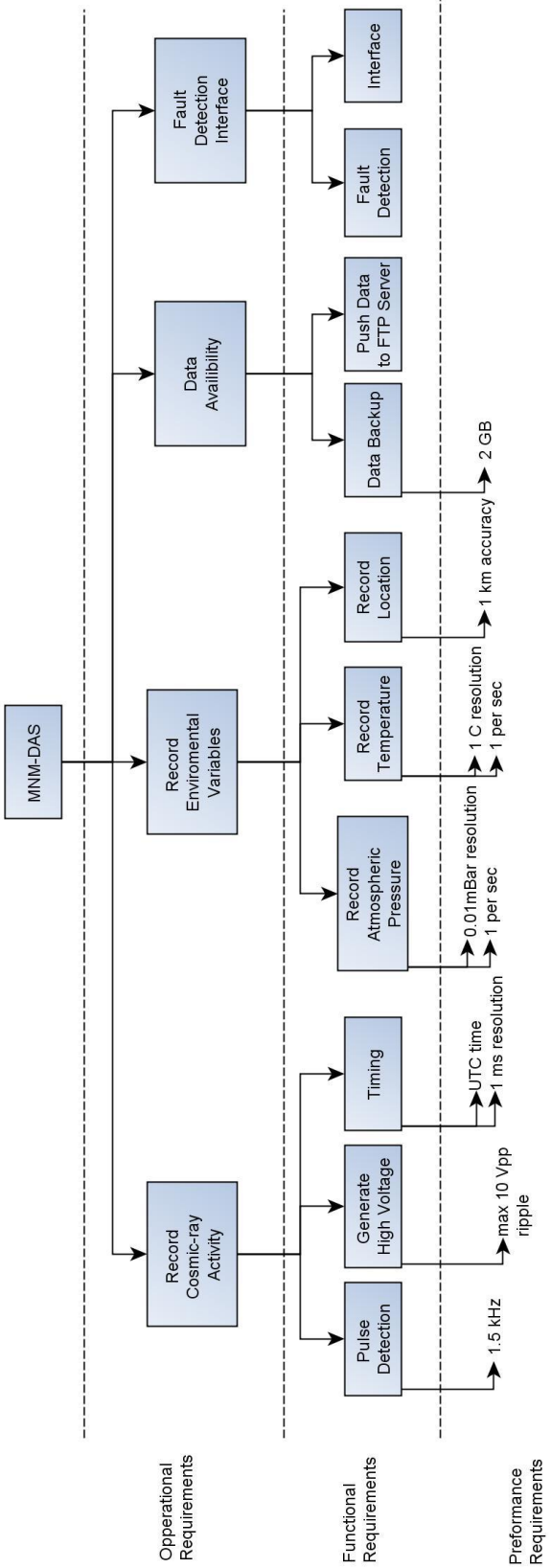

Figure 3-3: Objectives tree of the MNM-DAS

3.2.1 Operational requirements

There are four high-level functional requirements for the MNM-DAS. Operationally the requirements are the same as the requirements for the calibration monitor created in 2003, viz. to:

1. Detect and record cosmic-ray activity;
2. Record appropriate environmental variables;
3. Have recorded data readily available;
4. Preform self-diagnostics.

3.2.2 Functional requirements

There are ten distinct lower-level functional requirements that the system must meet in order to fulfil the high-level functional requirements. These are to:

1. Do pulse detection;
2. Generate high voltages in order to operate a proportional counter;
3. Synchronise system time with UTC time;
4. Record atmospheric pressure;
5. Record temperature;
6. Record the location of the system;
7. Save data on a FTP server;
8. Have a data backup system;
9. Do fault detection;
10. Have a human interface for fault detection.

3.2.3 Performance requirements

The performance requirements describe how well the above functions should perform their tasks.

1. Recorded pressure should have an accuracy of 0.01 mbar;

2. Pressure measurement should take place every second;
3. Recorded temperature should have an accuracy of 1℃ between 10℃ and 30℃;
4. Temperature measurements should be taken every second;
5. Location should be recorded within a one-km radius;
6. The generated high voltage should have a maximum ripple voltage of 5 Vpp;
7. Pulses down to 0.5 mV should be detected;
8. The system should be able handle a pulse train of up to 1.5 kHz;
9. Secondary storage space should be at least 2 GB.

3.2.4 Physical requirements and constraints

There are specific constraints that influenced the conceptual and detailed design of the MNM-DAS, as listed below:

- Physical size – operational;
- Logistical support – operational;
- Component availability – development;
- Project development time – development;
- Project cost – development and manufacture.

The first constraint that had to be taken into account was the physical size. The MNM-DAS must be able to fit into a space 40 cm wide and 20 cm deep. This is to enable the new equipment to replace the existing NM64 and calibration monitor without having to modify existing structures.

Logistical support was a major aspect of this project that had to be considered. The system had to be transported to SANAE using existing infrastructure. Since the first prototype had to be developed at SANAE, component availability was a major constraint. There was a time constraint on the research project as the duration from kick-off to termination was two years. Limited financial resources implied that development and equipment cost had to be kept to a minimum.

3.3 SYNTHESIS OF CONCEPTUAL SYSTEM DESIGN

In this section the synthesis of the conceptual design and architecture is discussed.

3.3.1 System architecture

The system architecture provides a functional definition in the form of functional units and an interconnection diagram for the unified system, as provided in Figure 3-4. The functional architecture for most neutron monitors should be similar as this is a generic "blueprint" for a neutron monitor.

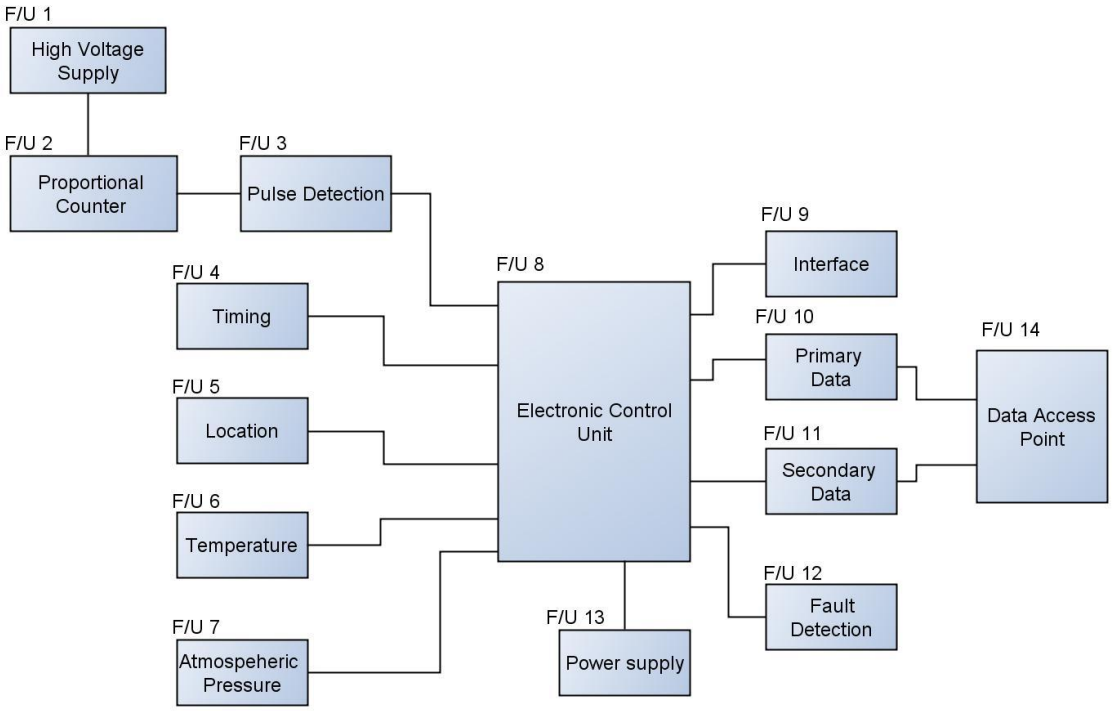

Figure 3-4: Functional architecture of the MNM-DAS

At the core of the system architecture is an electronic control unit (F/U 8). This is the functional unit that interconnects all functional units. In the case of the calibration monitor discussed in Section 2.2 on page 17, F/U 8 was an embedded PC. For the NM64 registration system currently used at the CSR, F/U 8 is a desktop PC.

The physical dimensions and gas used in the proportional counter (F/U 2) may differ between counter tubes; however, the principle remains unchanged. The counter tube will always require a high-voltage source and will generate a pulse when a secondary particle enters the system. This pulse will require amplification and pulse shaping (F/U 3) to register a pulse. The typical expansion of F/U 3 is shown in Figure 3-5 [**11**].

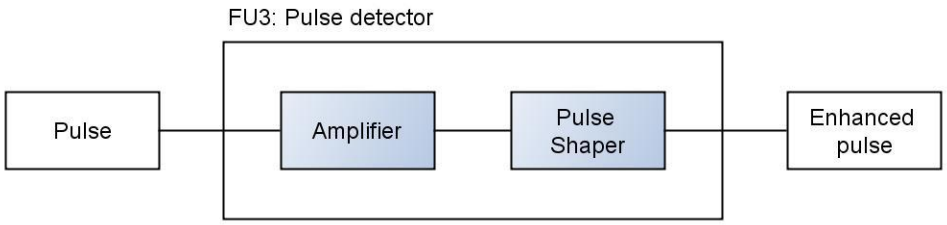

Figure 3-5: Pulse detector (F/U 3)

To form part of the NMDB (as discussed in Section 2.1.1 on page 8), a neutron monitor needs to synchronise its time on UTC time. For this, a real-time reference (F/U 4) is required.

All neutron monitors should record three environmental variables, namely (i) location (F/U 5), (ii) temperature (F/U 6), and (iii) pressure (F/U 7).These variables influence readings and must be taken into account.

Another important factor is fluctuations in high voltage. Therefore, a typical high-voltage supply definition is given in Figure 3-6. This is to limit drift in the high voltage, preventing it from operating outside the proportional region of a specific counter tube.

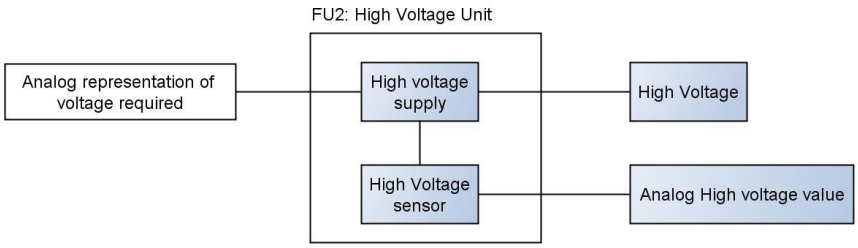

Figure 3-6 High-voltage unit (F/U 1)

A neutron monitor requires a human-machine interface (HMI, as defined by F/U 9) through which a user can interact with the system. This architecture is shown in Figure 3-7.

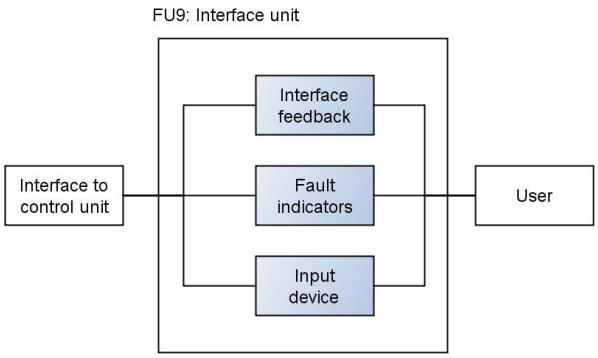

Figure 3-7: Interface unit (F/U 9)

A neutron monitoring system always has a primary storage (F/U 10) mechanism and a secondary data (F/U 11) storage mechanism to ensure data availability and integrity. Data from the device needs to be uploaded to the NMDB, which necessitates the presence of a data access point / interface (F/U 14).

3.4 ANALYSIS OF CONCEPTUAL SYSTEM DESIGN

A resource allocation is done to verify that the preliminary architecture makes provision for all requirements and to show which functional units are responsible for executing each high-level function.

Operational requirement	F/U 1	F/U 2	F/U 3	F/U 4	F/U 5	F/U 6	F/U 7	F/U 8	F/U 9	F/U 10	F/U 11	F/U 12	F/U 13	F/U 14
O/R1: Record environmental variables				x	x	x	x	x		x	x		x	
O/R2: Record cosmic ray activities	x	x	x					x		x	x		x	
O/R3: Data availability										x	x			x
O/R4: Self-diagnostics								x	x			x		

Table 3-1: Operational requirement resource allocation

Module functional requirements	F/U 1	F/U 2	F/U 3	F/U 4	F/U 5	F/U 6	F/U 7	F/U 8	F/U 9	F/U 10	F/U 11	F/U 12	F/U 13	F/U 14
F/R1:Record pressure							x	x		x	x			
F/R2:Record temperature						x		x		x	x			
F/R3: Record location					x			x		x	x			
F/R4:Generate high voltage	x							x		x	x			
F/R5:Detect pulse	x	x	x	x										
F/R6:Synchronise to UTC time				x										
F/R7:Have backup storage								x			x			
F/R8:Upload data to FTP real-time								x		x				x
F/R9: Automated fault detection								x					x	
F/R10: User interface								x	x					

Table 3-2: Functional requirement resource allocation

3.5 SUMMARY

In this chapter, the systems concept was synthesised based on the original functional definition of the registration system of the calibration monitor, as well as that of the registration system of the NM64 used at the CSR. The design started with a needs analysis of the existing and required system. It described the need identified in the environment in terms of high-level and lower-level functional and performance requirements. The system architecture was derived for the existing system and the required system by performing a functional analysis. The architecture describes the function and fit of each functional unit and how they interconnect to form an integrated system. A resource table described the resource allocation of each individual functional unit.

CHAPTER 4: PRELIMINARY AND DETAILED SYNTHESIS AND EVALUATION

4.1 INTRODUCTION

This chapter describes the detailed synthesis and evaluation of the MNM-DAS. The design of each functional unit, as provided in Chapter 3, is discussed in this chapter. This chapter provides detail at component level and describes the "how" of each high level function's "what".

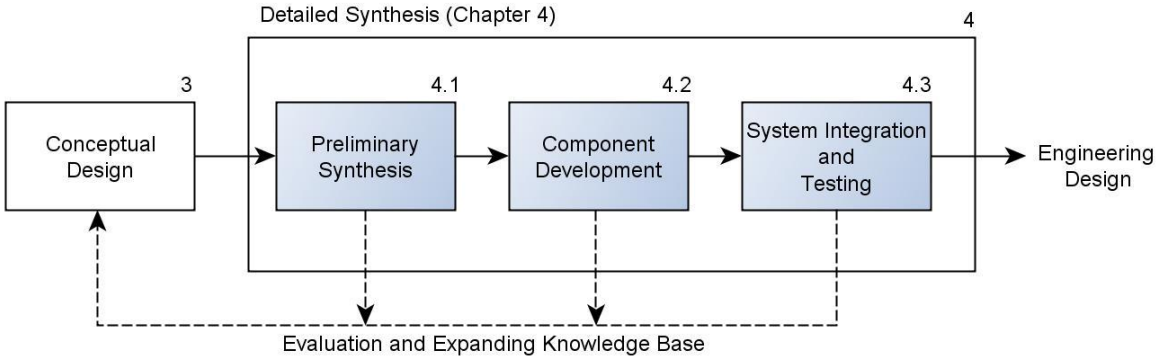

Figure 4-1: Preliminary and detailed synthesis phase

Figure 4-1 shows the process flow of the detailed synthesis performed in this chapter. The conceptual design produced in Chapter 3 was used as input requirements to this chapter to synthesise the preliminary system model. Thus, each component was selected according to requirements set out in the needs analysis and by taking all constraints into consideration.

Critical components were chosen using a multi-criteria decision-making (MCDM) process. Once all the components had been selected, modules were designed, built and tested, individually at first, after which the system was integrated and tested in its entirety. Integration was done with the use of a CAD programme to ensure mechanical fit, EMC, and mechanical rigidity and robustness.

4.2 PRELIMINARY SYNTHESIS

The preliminary functional architecture of the MNM-DAS is shown in Figure 4-2.

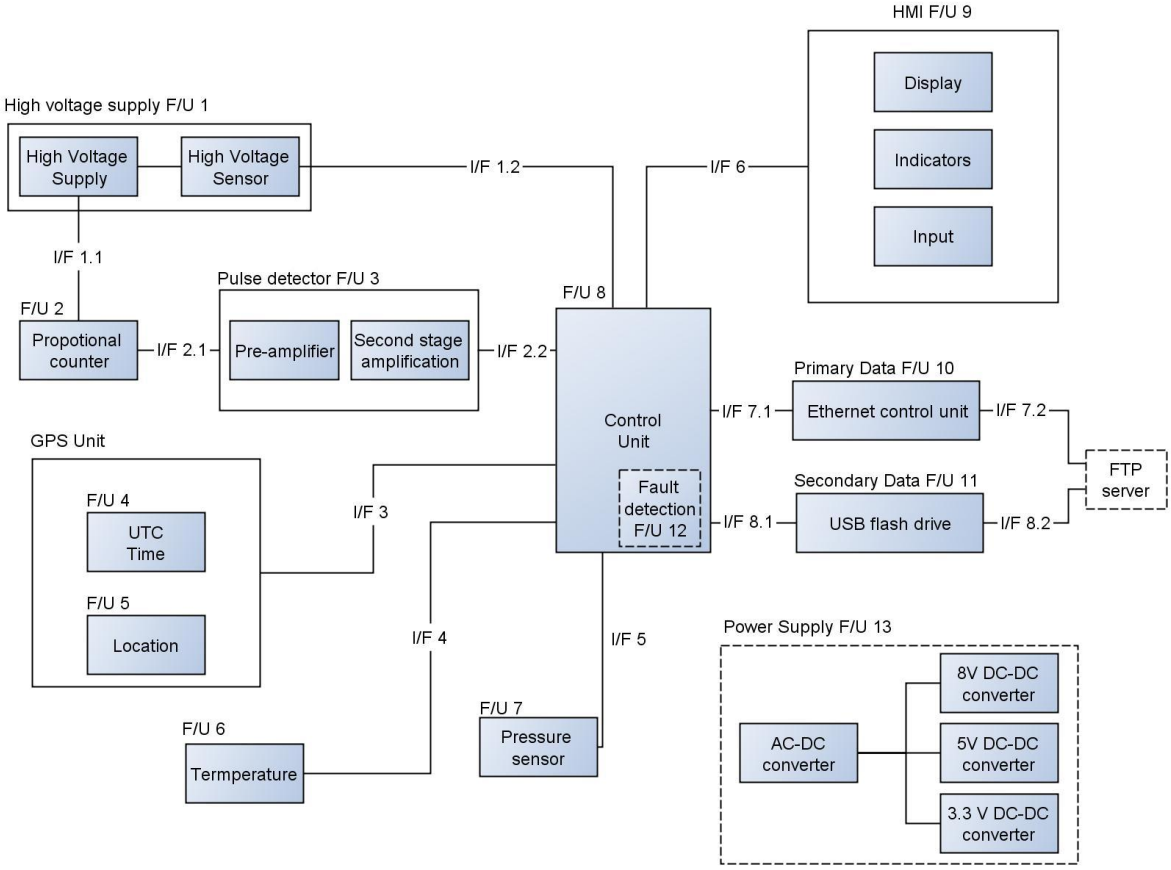

Figure 4-2: Preliminary functional architecture

The preliminary design phase resulted in a functional architecture at a low level and all interfaces that interconnect to low-level functional units. This intermediary level of abstraction provides a critical link between the high-level system concept and the component level (detail level) without losing generalisation. Therefore, future systems should be able to refer to the preliminary architecture without a loss of system integrity. That is, the functional architecture should not change, but components and modules may change in physical form. This is an example of the value of systems engineering in the design science research cycle as the functional architecture increases the body of knowledge in this context.

The logical order of design flow (i.e. design sequence) was as follows:

1. Control unit: The unit that implements the most functionality (by means of on-board hardware, interfaces, and firmware) was selected first to ensure functional capability, while taking into account design constraints such as availability, support tools, physical size and cost. Once the control unit had been completed, the signal flow determined the sequence of the design process, which is logical;
2. High-voltage supply and sensor: The unit that provides signal input to the system (and also had the most stringent size constraint) was completed next;
3. Pulse detector: The logical sequence of processing dictated that the pulse detector had to be designed after the high-voltage source had been completed as the input to the pulse detector is determined by the proportional counter output;
4. Time and location: Pulses must be time-stamped. As a result, once the pulse detector had been completed, time and location meta-data had to be added to the telemetric pulse data;
5. Sensors (temperature and pressure): Additional telemetric data includes temperature and pressure as these environmental variables influence the pulse rate. Corrections are made on account of this information as part of post-processing at the CSR;
6. Human-machine interface (HMI): The HMI provides the user with the ability to visualise environmental variables and to assist with fault detection (diagnostics);
7. Data access point: Once data had become available for transmission, a logical next step was to transmit telemetric data to a central server for post-processing. Transmission of telemetric data is done using the data access point;
8. Power supply: This unit was designed at the end of the detail design phase as its requirements could only be determined once all other components have been selected.

Details on the selection and design of each of the above components are given in the sections that follow.

4.3 COMPONENT DESIGN

Once all the components had been selected, detailed engineering and design of each functional unit commenced. Each component was developed separately, and tested individually. The following section describes all design decisions made at component level.

4.3.1 High-voltage supply F/U 1

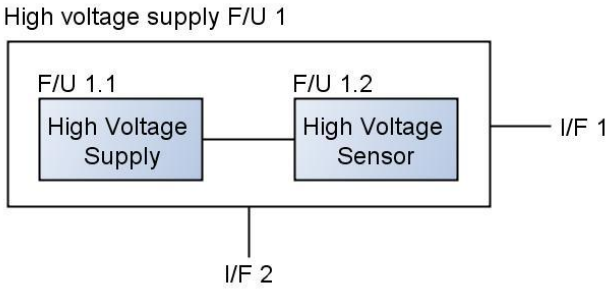

Figure 4-3: High-voltage supply F/U 1

The functional unit for the high-voltage supply is shown in Figure 4-3.

4.3.1.1 High-voltage supply F/U 1.1

In limited production run projects, such as this, it makes sense rather to buy specialized components than to build them due to high development cost and risk. Initial assessment revealed that attempts to develop a new high-voltage power supply would require a lengthy development time with sub-optimal performance as a result. The MCDM of this is shown in **Table 4-1**.

	Development time	Component cost	Component availability	Performance	Physical size	MCDM Score
	0.4	0.1	0.2	0.1	0.2	
New design	2	7	3	2	8	3.9
Commercial off-the-shelf	8	3	7	8	8	7.3

Table 4-1: High-voltage supply MCDM score

An increase in development time increases the total cost of the project and introduces a project development time risk. It is clear from the table above that development cost and risk outweigh the cost of a specialized commercial-off-the-shelf (COTS) component. The decision was made to use a COTS module, of proven reliability, for the high-voltage supply. The decision was made to use a Spellman MMP 5P1.5/12 high-voltage supply. Although different brands were available the CSR felt most comfortable with Spellman as they have been using them for more than a decade. This model is capable of providing an output voltage of 0 V to 5000 V linearly related to, and controlled by, inputs voltages of 0 V to 12 V. The specified maximum ripple voltage on the output is 0.2 % of the voltage, which gives a maximum ripple voltage of 4.8 V at an output voltage of 2400V. This input voltage was controlled using the circuit shown below in Figure 4.3.

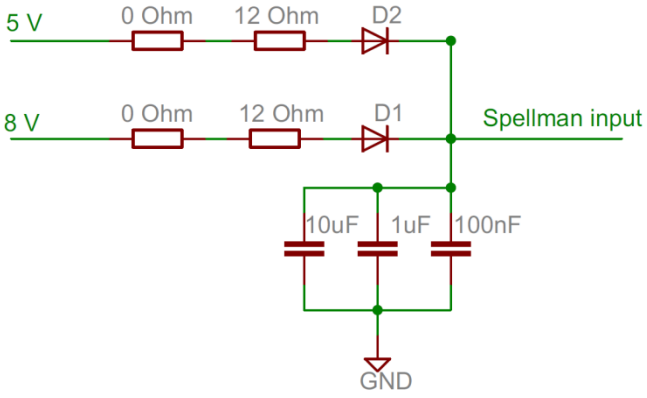

Figure 4-4: Voltage regulation circuit

For output voltages of 0 to 2000 V, the 5 V input line was used and for voltages of 2000 V to 4000 V, the 8 V input line was used. The shunt resistor selects the relevant control line during manufacture. By adjusting and then setting the secondary resistor (the 12 Ohm resistor in the control line above) the appropriate voltage was obtained. The example in Figure 4-4 will thus provide 1470 V if the 5 V line is used and 2400 V if the 8 V line is used.

Figure 4-5: High-voltage power supply

A photograph of the Spellman high-voltage power supply is shown in Figure 4-5 along with the PCB layout for the regulation circuit.

4.3.1.2 High-voltage sensor F/U 1.2

As shown in Figure 2-7 on page 16, the high-voltage source influences the counting rate of the proportional counter. A sensor is thus needed to measure the high-voltage values as input to a controller that limits drift or spikes that cause inaccurate data acquisition. The MCDM for this component is shown in **Table 4-2**.

	Development time	Component cost	Component availability	Performance	Physical size	MCDM Score
	0.4	0.1	0.2	0.1	0.2	
New design	4	5	9	6	5	5.5
Commercial off-the -shelf	6	5	2	4	5	4.7

Table 4-2: High-voltage sensor MCDM scores

To design a high-voltage divider is a simplistic and cost-effective task as it yields acceptable performance with minimal development time.

The high-voltage sensor uses a voltage divider network as shown in Figure 4-6. It uses a 20:1, followed by a 50:1 divider to give a 1000:1 voltage divider, meaning that for a high-voltage input of 2400 V, the divider has an output of 2.4 V, which is in an acceptable range for the on-board analogue to digital converter (ADC) of the micro-controller. Noise on the supply lines may cause incorrect readings that are amplified by a factor 1000 due to the conversion. Therefore, proper filtering of the supply lines (and suppression of other potential noise sources) was necessary – this was achieved by using decoupling and EMC guidelines, as given in [**16**].

The circuit diagram for the high-voltage divider is shown in Figure 4-6.

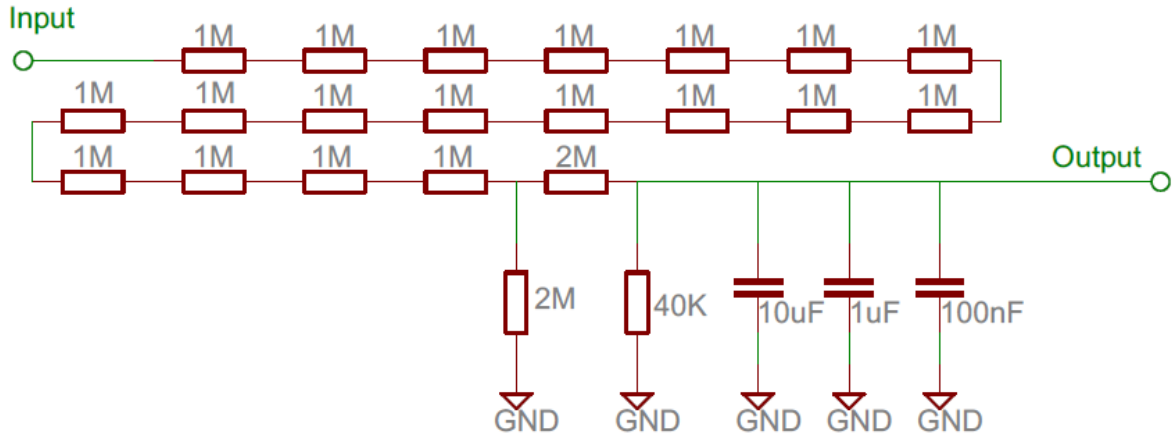

Figure 4-6: High-voltage divider network

The PCB layout of this circuit is shown in Figure 4-7.

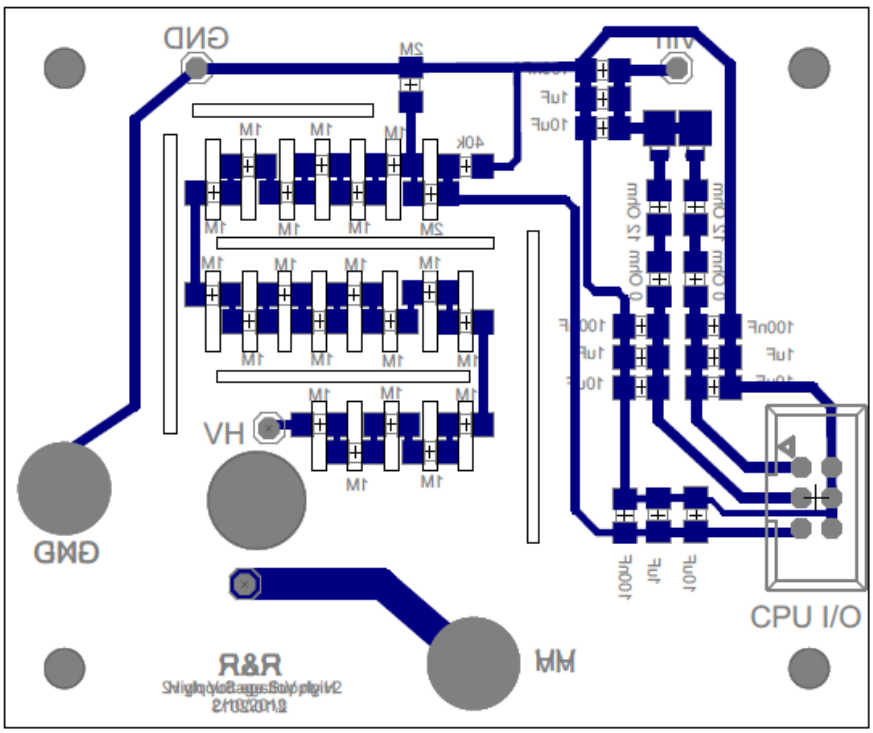

Figure 4-7: PCB layout of high-voltage divider network

Care should be taken when designing high-voltage circuits. The dielectric breakdown of dry air is 3.3 kV per millimetre between two spherical electrodes [**16**]. However, this distance is reduced with sharp edges and moisture in the air. Thus, physical dimensions had to be taken into account when working with high voltage. The rule of thumb is that for

every 1000 V between two planes, the minimum separation distance is 1 mm. This is important when building a divider as the arcing distance increases if it runs across a potentially conducting surface, for instance a PCB board. Dust, or other deposits on a surface, can reduce the isolation between high and low voltage nodes, which may cause arcing. Therefore, the circuit layout was done in such a way that no resistor has more than 150 V across it, which is the maximum working voltage allowed for 1206 surface mount packages. The resistor layout was also done in the form of an 'S' to maximize the distance between the differential planes with physical voids between the lines. This is illustrated in Figure 4-7.

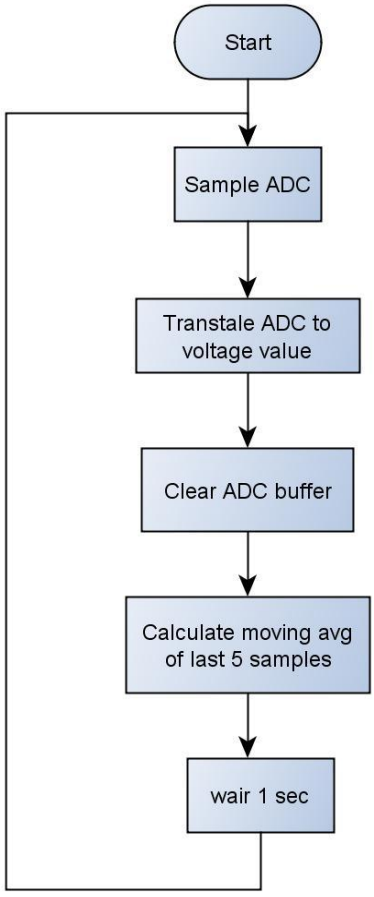

Figure 4-8: High-voltage sensor flow diagram

The operational flow diagram is shown in Figure 4-8. Using the micro-controller's built-in ADC, the voltage output from the divider network is sampled. The value obtained, along with a pre-set calibration value (stored on flash drive), is used to calculate the voltage

present on the high-voltage side. To further reduce the effects of noise, a moving average is calculated from the last five samples, with one second intervals between samples.

4.3.2 Proportional counter F/U 2

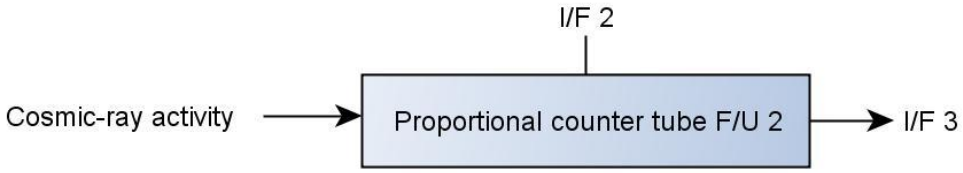

Figure 4-9: Proportional counter tube F/U 2

The MNM-DAS system is capable of interfacing with all He_3 or $^{10}BF_3$ proportional counter tubes. When implementing these tubes, it is necessary to pre-set the high voltage to the correct level for operating in the proportional counting region (Figure 2-7 on page 16). This can be done by controlling the high-voltage source as discussed in section 4.3.1.1.

4.3.3 Pulse detector F/U 3

Cost constraints prevented the use of a COTS amplifier for the pulse detector unit, which necessitated a new design. Although an in-house development was underway to design a new pre-amplifier (refer to work of Stefanie Strachan [**17**]) it was unfortunately not available at the time of production, and a new design was done.

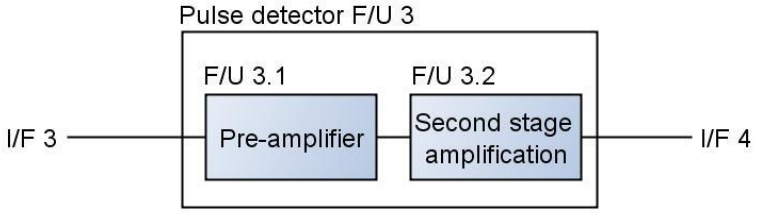

Figure 4-10: Pulse detector F/U 3

The functional flow diagram of the pulse detector is shown in Figure 4-10. The detection can be divided into two parts, namely (i) a pre-amplifier and (ii) a second stage amplification and filtering network.

4.3.3.1 Pre-amplifier F/U 3.1 & second stage amplification F/U 3.2

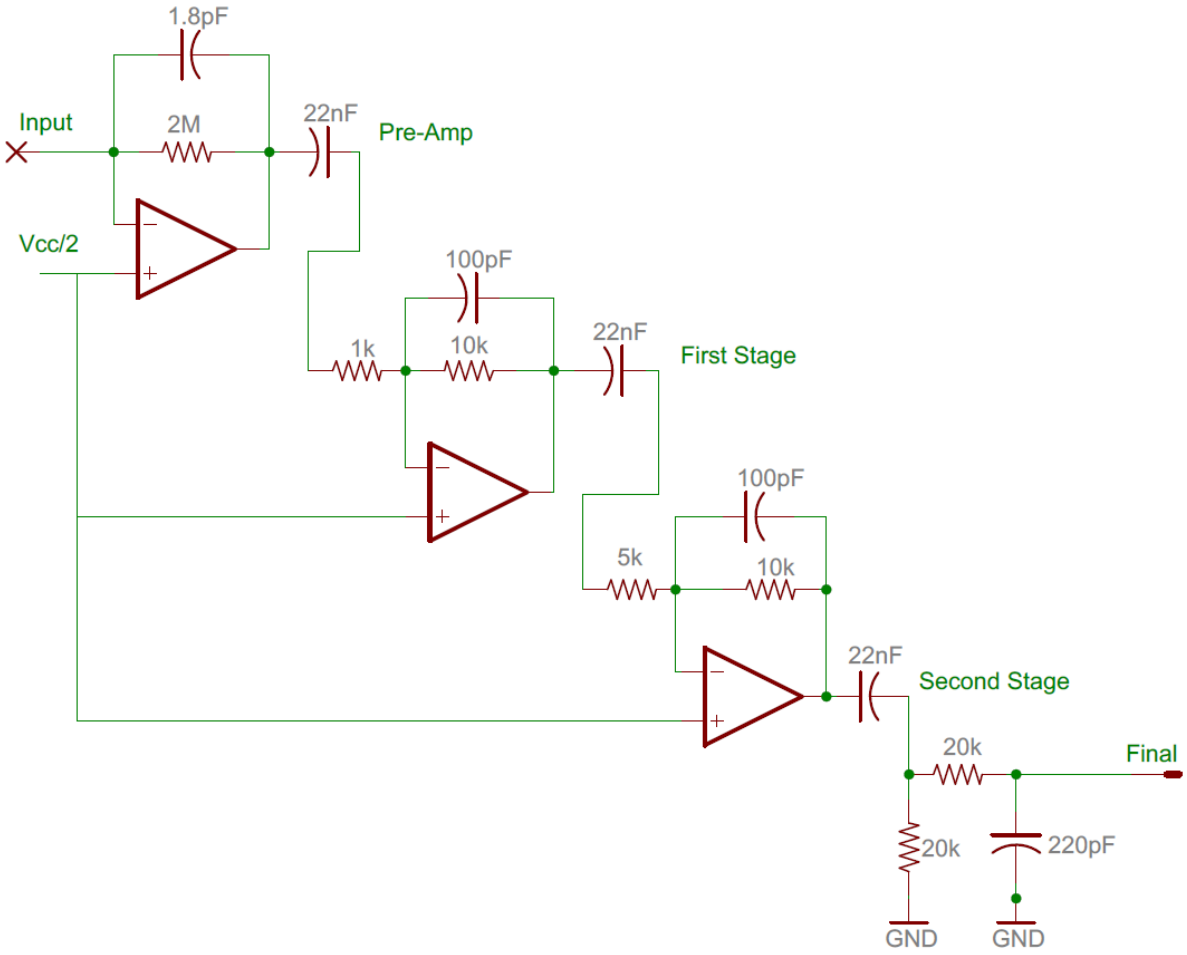

Figure 4-11: Pre-amplifier circuit

The pre-amplifier uses a basic charge-sensitive amplifier as depicted Figure 4-11. This is followed by two stages of amplification and a final filter stage.

After the pre-amplifier stage, pulses are still too small to be sampled and discriminated by the controller. The circuit above uses two inverting charge amplifier circuits and a band-pass filter to amplify the pulse and to filter out noise. The respective responses of the amplifier stages are shown in Figure 4-12 and Figure .

The frequency content of the pulses generated from a proportional counter tube ranges up to 100 kHz. This is where the transfer function of the pre-amplifier stage is at its peak, as shown in Figure 4-12.

The phase difference as phase delay does not play a role in pulse detection for the MNM-DAS. The phase transfer is included for the sake of completeness in Figure 4-13

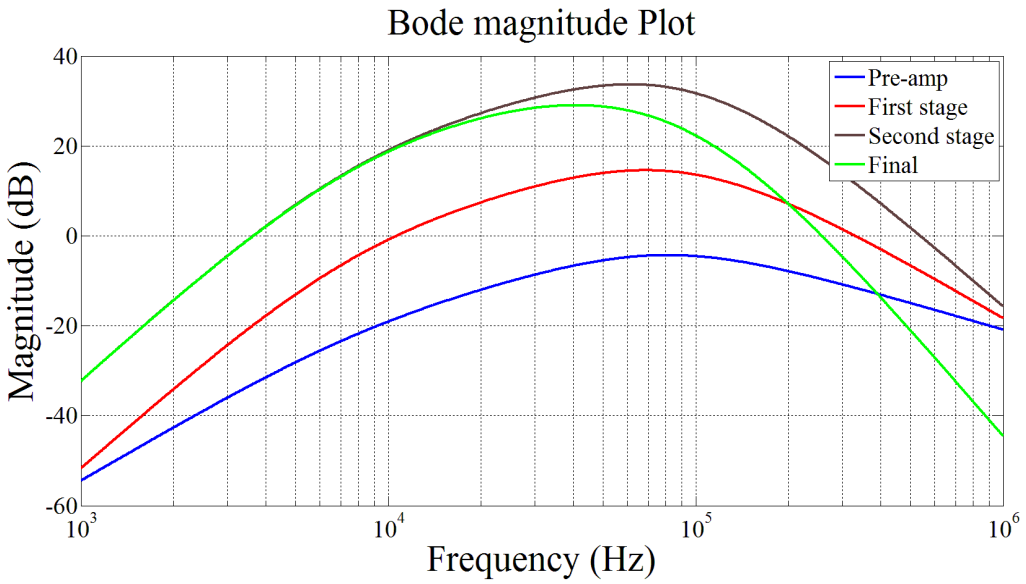

Figure 4-12: Bode magnitude plot

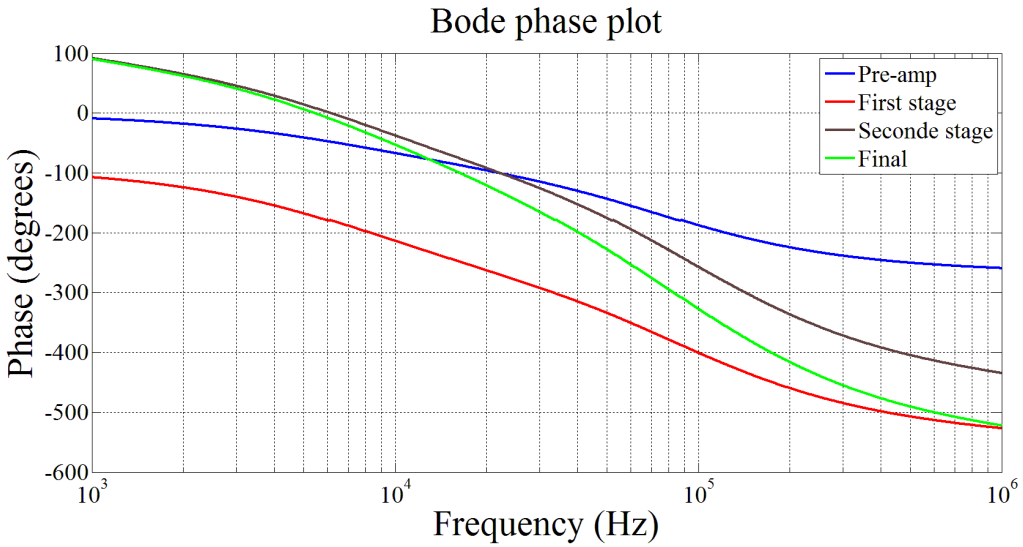

Figure 4-13: Bode phase plot

Figure 4-14 shows a photograph of the pre-amplifier and high-voltage decoupling capacitors. The capacitors were placed in such a way that possible arcing between them is minimized and spacers to separate the two PCB boards apart are of non-conducting plastic. The circuit on the bottom PCB (Figure 4-14) contains the high-voltage filters. The other end of each capacitor C1 to C3 is connected to the ground of the pre-amplifier PCB.

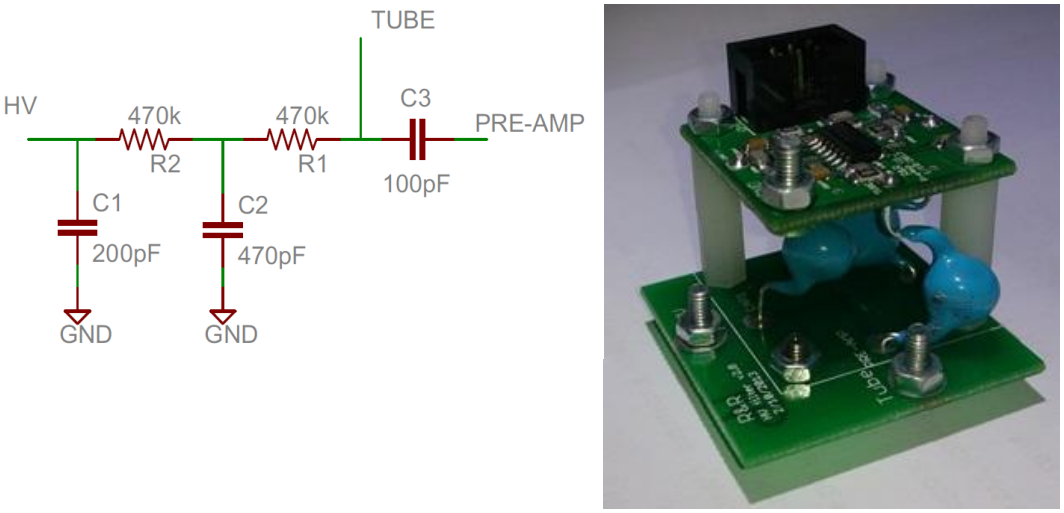

Figure 4-14: a) Circuit diagram of high-voltage filter network, b) Photograph of pre-amplifier and high-voltage decoupling capacitors

4.3.4 Real-time and location F/U 4 & F/U 5

There are various methods of tracking real time, including a GPS real-time source, or an NTP server clock chip. However, there is only one feasible way of providing reliable location information at a remote location such as Antarctica. The GPS system was selected to realize F/U 4 as it provides both real time and location data.

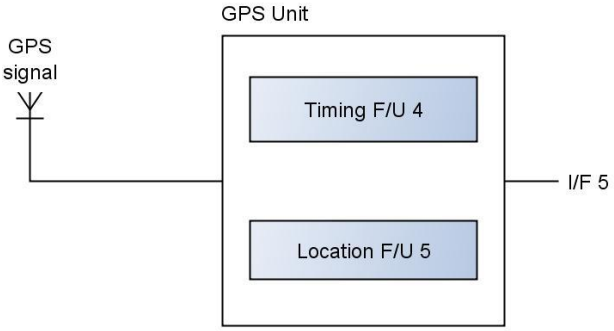

Figure 4-15 GPS F/U 4 & F/U 5

The GPS module is a COTS module from a well-established product supplier (LEA-6/NEO-6 u-block). As the MNM-DAS is an indoor unit, indoor reception became a requirement. Hence an active antenna was selected to improve reception. The selected U-Block module is supplied as standard with a 12 V UART interface (standard EIA-232). To provide electrical compatibility between the controller and the GPS module, the EIA-232 level converter IC was bypassed on the GPS module to provide TTL levels. Figure 4-16 outlines all the modifications.

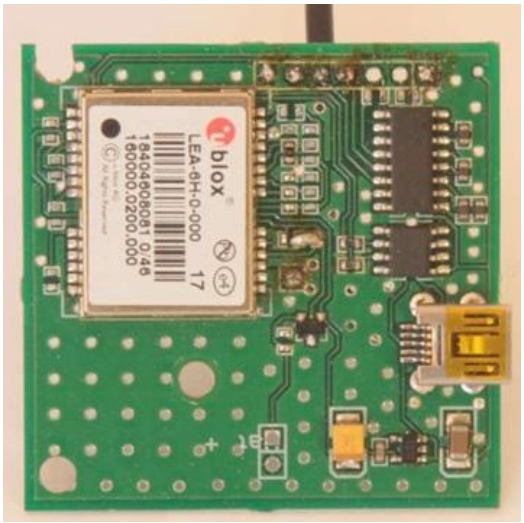

Figure 4-16: GPS module modifications

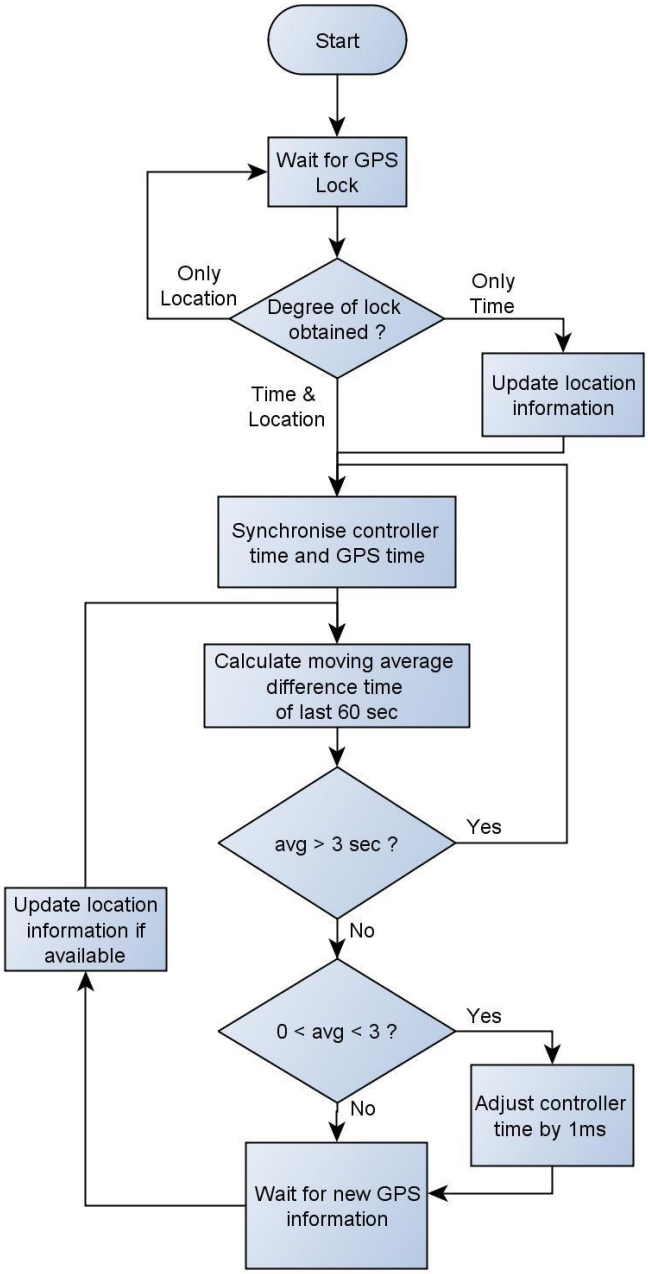

Figure 4-17 : GPS firmware flow diagram

Figure 4-17 shows the program flow diagram of the process the micro-controller follows to obtain GPS data.

The controller waits for the module to obtain a lock before data registration takes place. Depending on the satellite coverage in the area, the signal may be sufficient to obtain time, but not location. The micro-controller synchronises its own time and date with those of the GPS module. It then calculates the difference in time of the module and its own on-board time. This is done using a 60-second moving average. If the moving averages of the two time sources differ by more than three seconds, the controller resets the GPS module time. If the moving averages differ by less than three seconds, the controller adjusts its own time by one ms per second. With this process in place, the controller is able to adjust time without disrupting the data by up to three seconds of drift in an hour, which is acceptable. A moving average was used because of GPS scintillation (i.e. time delays due to atmospheric conditions) as well as time delays in processing incoming data from the GPS.

4.3.5 Temperature sensor F/U 6

A 5 kΩ 1 % radial thermistor was used for temperature sensing. The transfer function of the thermistor is not linear over its whole range, but the temperature region in which the sensor operates is sufficiently linear for this system.

A 20 second moving average was used to filter out noise, with a sampling interval of 1 second.

4.3.6 Pressure sensor F/U 7

The pressure sensor that was selected is a Paroscientific pressure sensor. These pressure sensors provide better pressure performance than 0.01% of full-scale pressure. This translates to an accuracy of 0.01 mbar in the range of operation of this application. The sensor uses a 12 V EIA-232 connection set at a rate of 19200 bits per second and was set up to broadcast pressure every second.

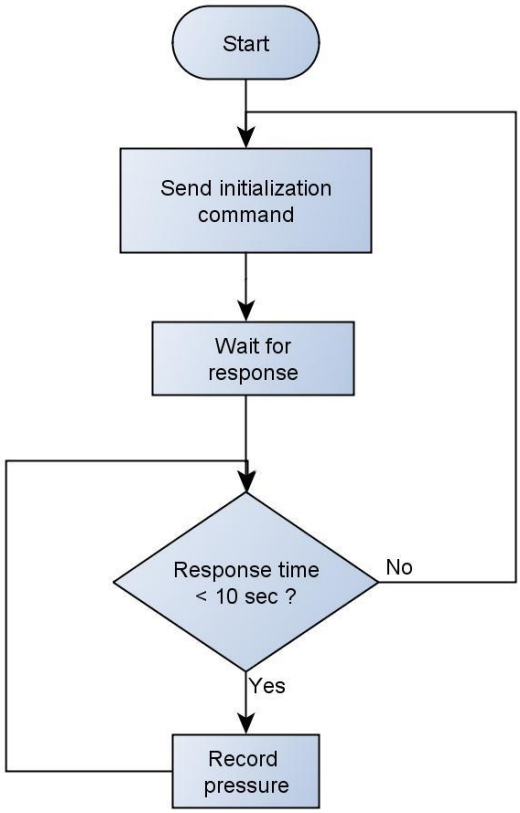

Figure 4-18: Pressure firmware flow diagram

This specific unit was chosen as the CSR already had these sensors and the sensors meet the requirements defined in Chapter 3. A MAX232 level conversion IC was used to interface with the controller.

The operational flow of the firmware processing incoming pressure data is shown in Figure 4-18. An initialisation command is sent to the pressure sensor to start transmitting pressure data. The pressure sensor sends pressure data every second. The micro-controller waits for ten seconds for pressure data to arrive. If this does not take place, the controller will re-initialize the pressure sensor. This will continue until pressure data has been received. The re-initialization will happen any time the controller has not received data for more than ten seconds.

4.3.7 Electronic control unit F/U 8 & F/U 12

Table 3-2 on page 38 showed that the control unit is critical to the system. Careful selection of an appropriate controller will reduce risk and constraints associated with factors as shown in the MCDM table below, (**Table 4-3**).

	Development time	Component cost	Component availability	Performance	Physical size	MCDM Score
	0.4	0.1	0.2	0.1	0.2	
Micro-controller	8	8	5	3	8	6.9
Processor	3	6	5	8	8	5.2
Embedded computer	4	2	5	10	1	4

Table 4-3: Electronic control unit MCDM score

An embedded computer was disqualified from selection due to size constraints.

A general processor was disqualified due to the long development time as the required tools and firmware development support available to the team at the time were not adequate to finalize this development in time.

This left a general micro-controller as a viable option. A micro-controller option provided sufficient firmware development support, integrated peripherals and memory. Although the PIC controller had a lower performance score than the other two options, the controller met the requirements for this system. The selected micro-controller is the PIC32MX795 as it provided all the functionality required for the MNM-DAS.

The flowchart of the controller firmware is shown in Figure 4-19.

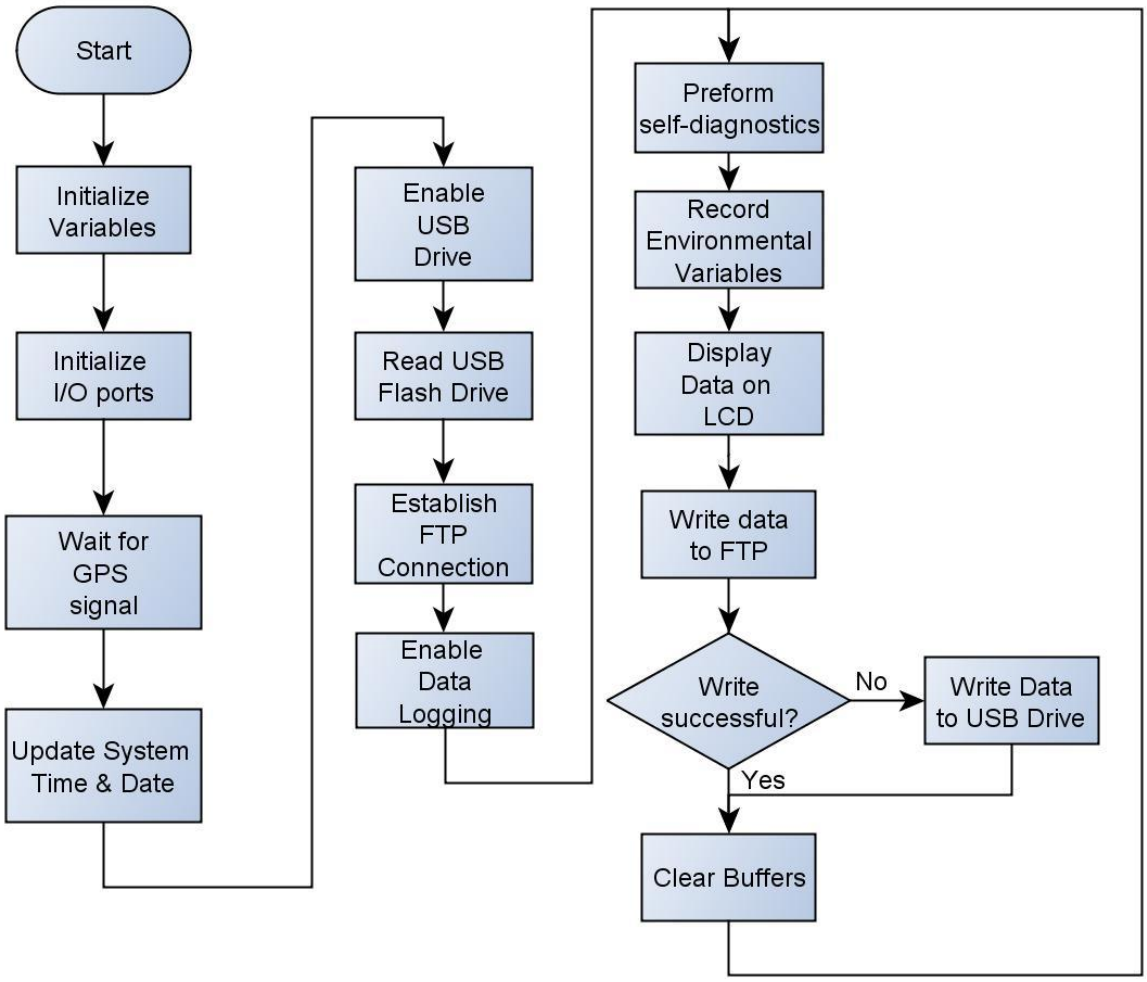

Figure 4-19: Control unit flow diagram

The micro-controller starts off by initializing all the required variables and all the I/O ports connected to the controller. The system then waits until GPS lock is obtained, after which the system time and date are updated. The controller will then enable USB communication and read the flash drive in order to obtain, among others, all the credentials for the FTP server. Using these credentials found in the configuration file the controller will open a FTP session to the FTP server. This completes the start-up process and data logging can commence. However, before data is recorded the system will perform a self-diagnosis to ensure all the systems are up and running. The environmental variables that can influence cosmic-ray activity is recorded and displayed on the LCD screen. Once the buffers are full they are written to the FTP server and cleared. However if this writing cycle fails the data

is written to the flash drive instead. There will be a five-second overlap of data to ensure that no data is corrupted during a network failure.

The code is based on an interrupt and during any time after the start-up procedure the system can be interrupted to take a time-stamp of an incoming pulse and then resume normal operation.

4.3.8 HMI F/U 9 & Fault management F/U 12

A photograph of the HMI is shown in Figure 4-20. Indicators on the HMI provide the operator (or technician) the ability to identify persistent faults that require repairs. The operational manual for the MNM-DAS is given in Appendix A.

Figure 4-20 : HMI

The display unit consists of a 20 x 4 LCD screen that uses an 8-bit parallel port for communication. There are five LED indicators that provide information on whether critical systems are running. The separate LED indicators indicate when (i) the system is running, (ii) GPS lock is obtained, (iii) an FTP session is open, (iv) a USB flash drive is mounted, and (v) the pressure sensor is connected. The display is navigated by the use of the UP and DOWN buttons on the front panel. There is also an eject button to allow for the flash drive to be safely removed and prevent data corruption on removal.

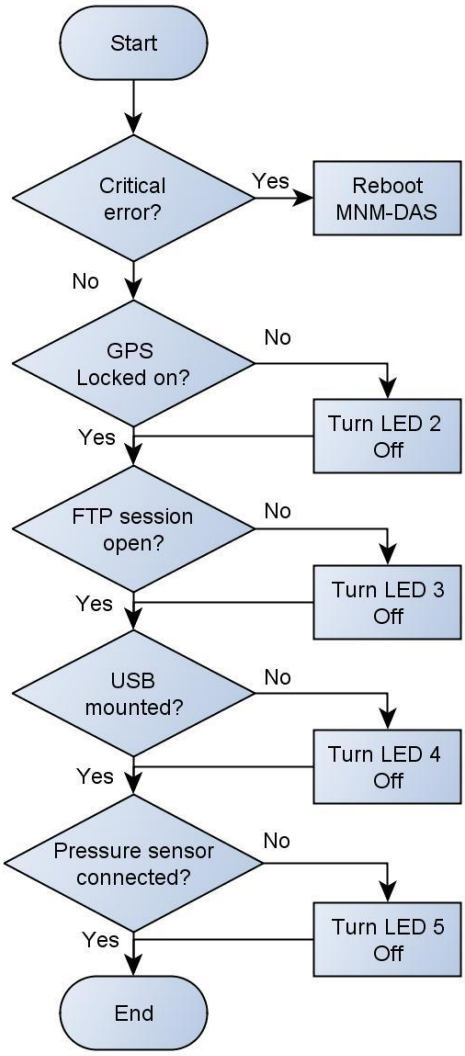

Figure 4-21 : Fault management flow diagram

Fault management is done mainly in software. The flow diagram for this management process is shown in Figure 4-21. The self-diagnosis starts off by checking whether there are any critical errors, for instance whether the flash drive is corrupt upon start-up; whether a critical error has been found, the MNM-DAS will reboot in an attempt to repair the error. If no critical errors have been found; the system will sequentially check the status of the GPS, FTP connection, USB flash drive and the pressure sensor. If one or more of these are experiencing a problem the appropriate LED indication will switch off.

4.3.9 Primary storage F/U 10

The current system requires the primary data storage unit to be hosted on an FTP server. This enables users who access data to access the neutron monitor data in real time from anywhere in the world, provided the FTP server is also connected to the internet. There were only two options at the time of the design, namely:

- To implement an FTP client on the micro-controller (F/U 8), or
- Buy a COTS module to implement an FTP client.

Figure 4-22: Primary data storage

The PIC32MX795 is capable of handling an Ethernet stack; however, due to the heavy processing load on the micro-controller from the rest of the functional units, the choice was made to use a COTS Ethernet module.

Ethernet traffic is handled with the use of an external module (Nano Socket LAN CO214). Communication to the chip is done with a UART connection. Using the UART connection,

commands can be issued to the chip in order to access the FTP server. However, the IP stack is handled by the Ethernet module.

Figure 4-23: Nano socket LAN

The operational flow of the primary storage unit can be seen on the flowing page in Figure 4-23. The monitor logs into the FTP server using a username and password with appropriate authentication on the system. The local administrator for the FTP server will handle authentication for the specific site. A file is created daily on the server with time stamps appended to the file each second along with environmental variables. If a connection is lost, the system attempts to establish connection to the server every second. If the response time of the network is more than a second, a buffer will be used to queue data.

Using the username and password obtained from the flash drive, the monitor opens an FTP session. If successful, a directory is created. Consequently, a file is created using a date stamp as reference. All data is appended to the data file in a sequential fashion. All data will be committed to the data file until the data buffers have been cleared.

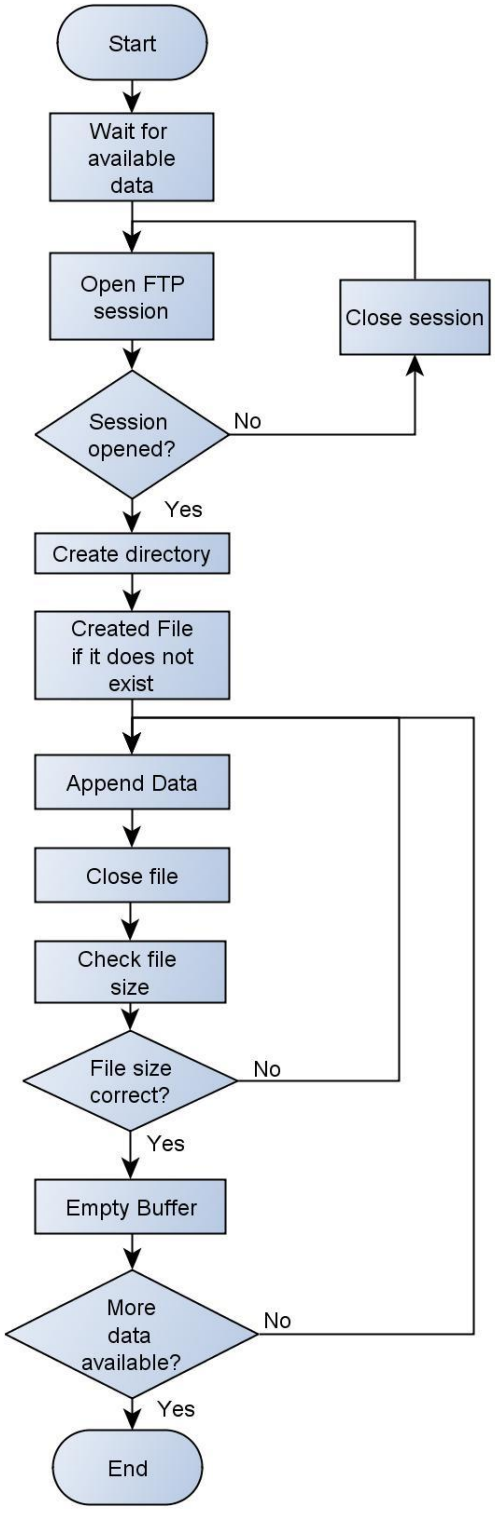

Figure 4-24: Ethernet flow diagram

4.3.9.1 FTP server

The FTP server does not form part of the scope of this project. However, for setup and demonstration purposes, the FTP server software was installed on a Linux server (Proftpd). This is not fixed and any FTP server can be used to connect as long as it provides the appropriate login authentication. The configuration of the MNM-DAS is done with a text file stored on the flash drive, containing IP addresses and subnet masks.

4.3.10 Secondary storage F/U 11

There were two options for a secondary storage unit that must be capable of handling the amount of data required, namely (i) a flash drive/external hard drive or (ii) an SD card. The flash drive was selected for its ease of loading and data access. USB ports are far more common than SD card readers. This also provides the capability to connect either a flash drive or an external hard-drive. The flash drive was also selected because of its lower power consumption and smaller mechanical size.

The flash drive can be a generic flash drive as long as it supports a FAT32 file system with a sector size of 4025. The average file size generated by a MNM-DAS at sea level with a ^{3}He tube connecter is 415kB. However, it is 4 MB for the MNM-DAS connected to an NM64 at 800m above sea level in the Antarctic region. The device should be able to handle at least six months of downtime on the network to the FTP server. A 4 GB flash drive was considered to provide sufficient backup for a six month period.

A configuration file in the root directory contains login information of the FTP server, the high-voltage calibration value and settings for specific experiments. This file must be present at start-up so that the MNM-DAS can log into the FTP server. Once this file has been read, the flash drive can be removed, but has to be present for data backup.

The flash drive serves as secondary data storage. If FTP is unable to connect or falls out for more than five seconds, data is stored on the flash drive until a new session has been established (see the Figure 4-24 below for the functional flow of this storage procedure).

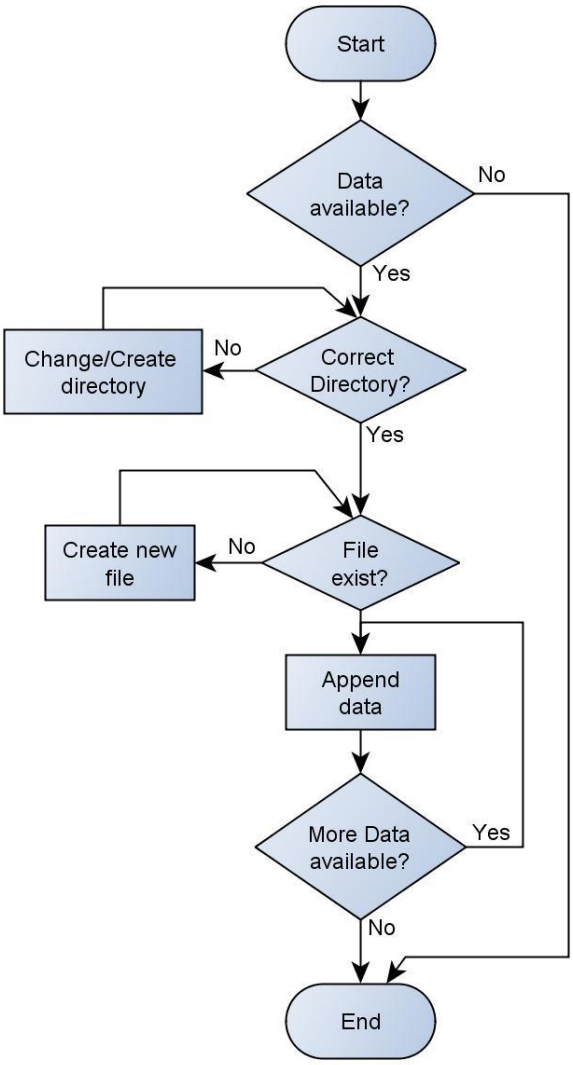

Figure 4-25: Writing to the USB flash drive functional diagram

As soon as the system detects a problem with the FTP server, it falls back to USB storage. It creates a directory of the year and month if it does not exist. A text file using the day and year is created. Data is not sent in one packet. In order to do multi-threading and not hold up active processes, data is stored in packets. As soon as all the data has been transmitted, it is verified. The system will also only start writing to the flash when there is at least 10 seconds worth of data in the buffer. Should the FTP fail and only the flash drive be used, the maximum read/write cycles of a normal flash drive will be exceeded within the first

month. By using this technique the flash drive can last an average of 10 months before it could fail.

4.3.11 Power supply F/U 13

The power converter was designed in such a way that it can handle a range of 4 V to 6 V as input. This provides the power supply unit with a wide array of options to use as a 5 V input supply. The EDM is currently powered with an off-the-shelf cell phone charger that has an output of 5 V and a maximum current output of 1 A. This proves to be more than sufficient as the MNM-DAS uses only 500 mA. It uses a detachable USB to micro-USB cable. This option allows the MNM-DAS to be powered with a USB port as well as the power supply.

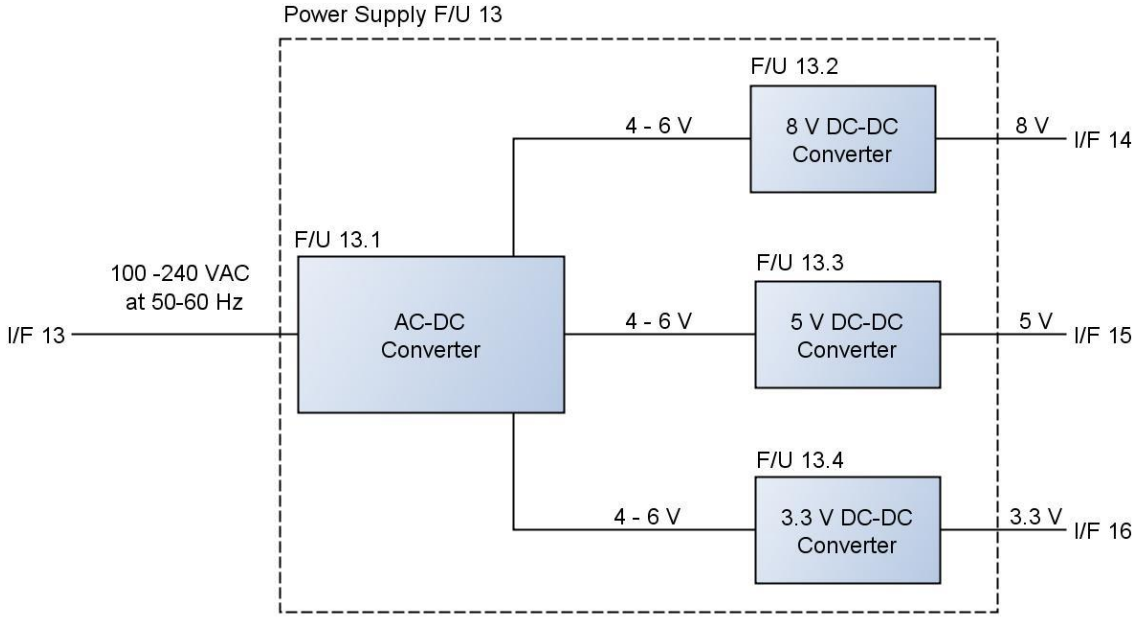

Figure 4-26: Power supply F/U 13

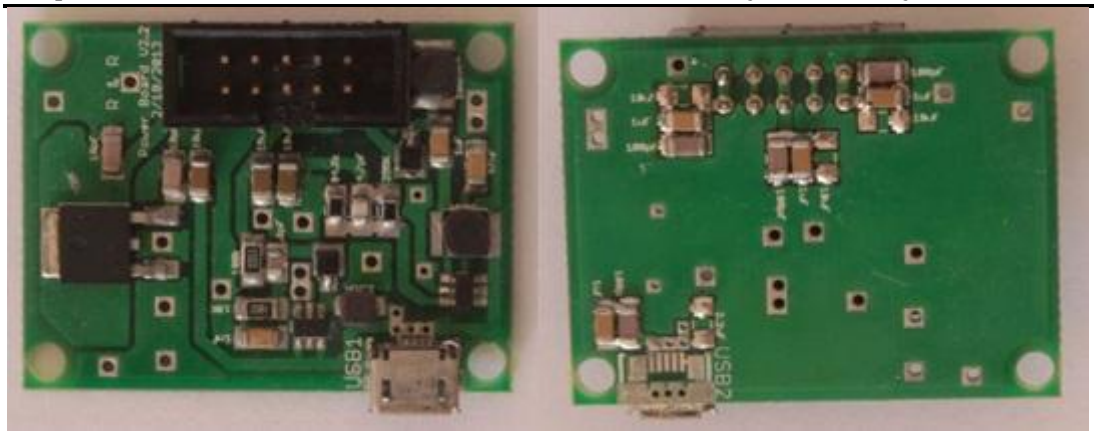

Figure 4-27: DC-DC converter

The voltage converter uses a micro-USB socket as input and an 8-pin dip-connector socket as output as shown in Figure 4-26. The micro-USB input socket makes the powering of the device versatile enough that it can even be powered with a USB port, if required.

	3.3 V output	5 V output	8 V output
Ripple voltage p-p	0.02 mV	5 mV	10 mV
Maximum current	1 A	1 A	1 A

Table 4-4: Voltage converter specifications

The voltage converter performance specifications are shown in **Table 4-4**. These specifications are valid provided the input voltage is 4 to 6 V.

4.3.11.1 AC -DC converter F/U 13.1

The average power consumption of each functional unit is given in **Table 4-5**. From this it is calculated that the total power consumption of the MNM-DAS is 2.11 W, meaning that the AC-DC converter F/U13.1 must be able to supply a current of 422 mA on the 5 V line.

	3.3 V	5 V	8 V
F/U 1: High-voltage supply			40 mA
F/U 3: Pulse detector	< 1 mA		

F/U 4 & F/U 5: GPS		70 mA	
F/U 6: Temperature	< 1mA		
F/U 7: Pressure sensor			4 mA
F/U 8: Micro-controller	200 mA		
F/U 9: HMI	10 mA	25 mA	
F/U 10: Primary storage		100 mA	
F/U 11: Secondary storage		18 mA	
Average power consumption	210 mA	213 mA	44 mA

Table 4-5: Power consumption of MNM-DAS

For the purposes of all the current installations, a 5 V cell phone charger capable of delivering a 700 mA current was used.

4.3.11.2 8 V DC-DC converter F/U 13.2

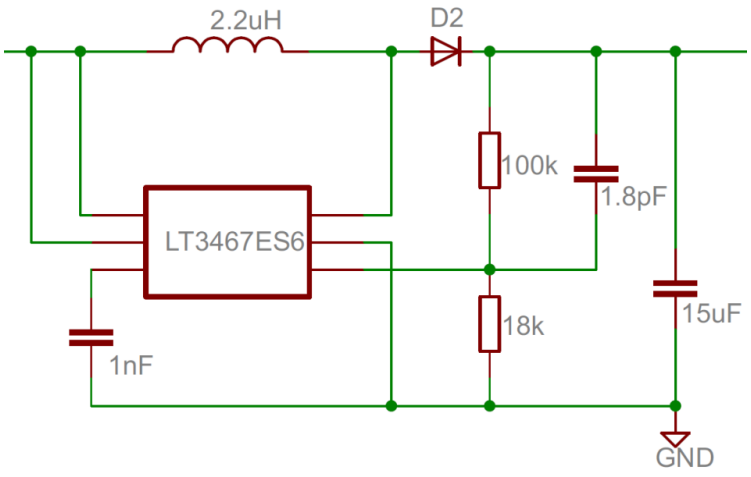

Figure 4-28: 8 V DC - DC converter circuit

The minimum operating voltage of the Paroscientific pressure sensor is 6 V but it can accept inputs up to 18 V. The required input voltage of the Spellman high-voltage supply is 0 to 12 V. However, to produce a high voltage of 2800 V, the input voltage must be 7.2 V. Thus the 8 V circuit shown in Figure 4-27 was designed to supply power to the Spellman

module. If more than 8 V is required by the high-voltage supply due to an increased voltage requirement by the proportional counter tube, the ratio of the 225 kΩ and 84.5 kΩ can simply be changed to produce the increased voltage.

4.3.11.3 5 V DC-DC converter F/U 13.3

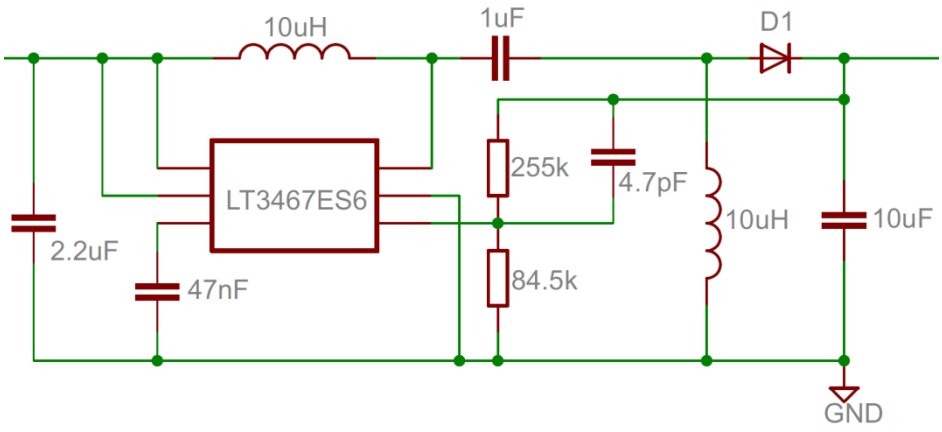

Figure 4-29: 5 V DC - DC converter circuit

The circuit shown in Figure 4-28 produces a 5 V DC output for an input range of 4 V to 6 V. This circuit cleans the 5 V input, which is used to power the MNM-DAS and extends the range of available options for F/U 13.1, as cell phone chargers provide an output range of 4.5 V to 5.5 V depending on make and model.

4.3.11.4 3.3 V DC-DC converter F/U 13.4

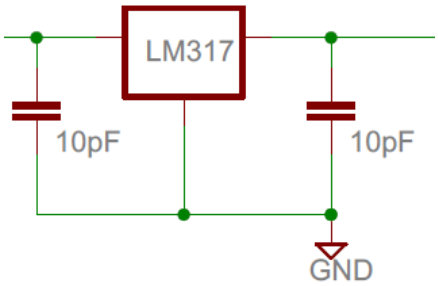

Figure 4-30: 3.3 V DC - DC converter circuit

The 3.3 V is generated with an LM317 linear regulator. This provides a stable 3.3 V to the micro-controller, pre-amplifier and Ethernet module.

4.4 SYSTEMS INTEGRATION AND TESTING

Once all the components had been selected, detailed engineering and design of each physical unit started. Each unit was developed, programmed and tested individually. A photograph of the component design phase can be seen in Figure 4-30.

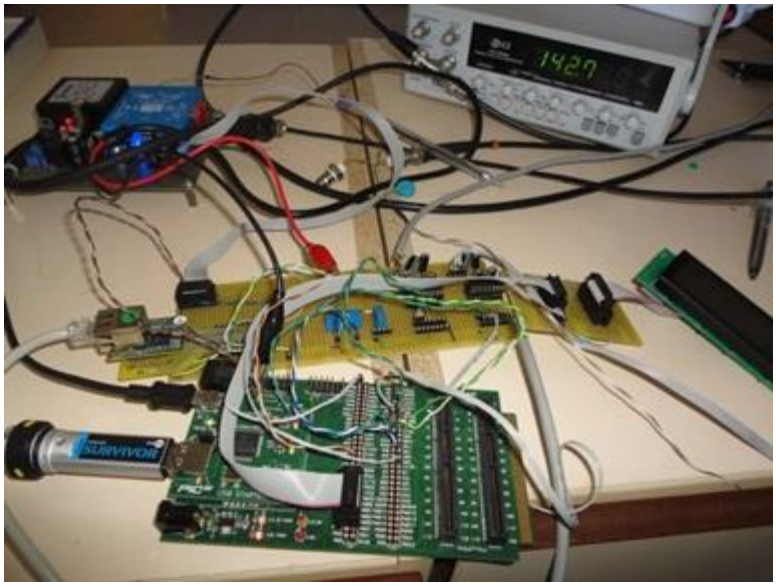

Figure 4-31: Component development phase

All the components were integrated on veroboard and a development expansion board as shown in Figure 4-30 to demonstrate functional capability and facilitate firmware debugging.

After all the components had been integrated and functional, they were drawn up in a CAD model to:

- Determine the physical placement of components;
- Minimize EMI;
- Reduce physical size; and

- Obtain safe working distances from the high-voltage wires.

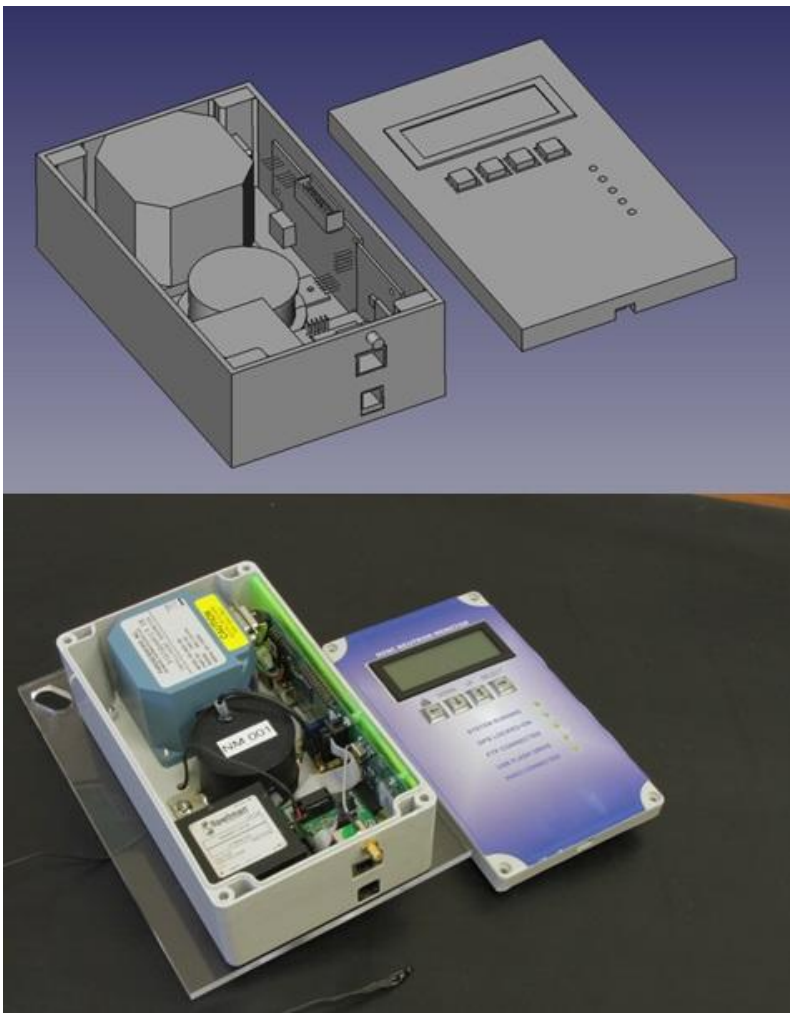

Figure 4-32: ADM CAD model and physical device

The advanced models have been running on Neumayer station as well as the Polarstern since December 2013. The Polarstern installation is shown in Figure 4-32 (a) and the Neumayer installation is shown in Figure 4-32 (b)

Figure 4-33: ADM (a) Polarstern and (b) Neumayer installations

4.5 ENGINEERING DEVELOPMENT MODEL (EDM)

This EDM is also the production version of the MNM-DAS; it was designed to be repeatable, robust and small. The major differences between the ADM, EDM, and production mode are:

1. The ADM demonstrates functional capability of new functions, where the EDM provides a model that also addresses all physical requirements;
2. In this research, the ADM was used to determine the physical arrangement of components, which was optimised in the EDM in the following iteration;
3. Manufacturability was considered in the EDM, and optimised in the production model.

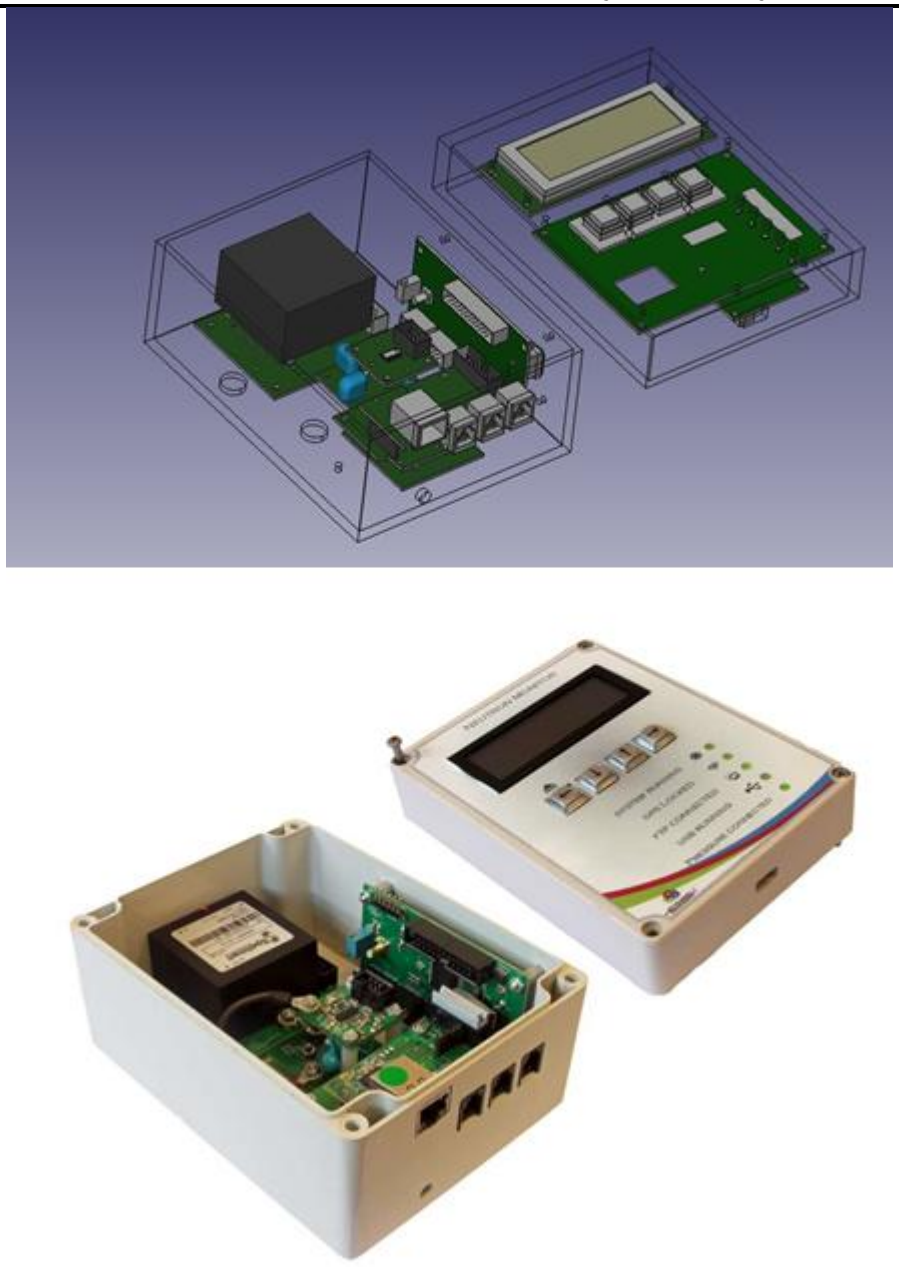

Figure 4-34: Engineering Development Model (EDM)

4.6 PRODUCTION

Figure 4-35: Production

Figure 4-36: SANAE installation

4.7 SUMMARY

In this chapter the preliminary design process was described to demonstrate how to obtain the proper function, fit (interfaces), and form for every functional unit in the systems architecture. The detailed development phase was discussed, where all functional units were addressed, and where design decisions and selections made according to constraints.

After all the components had been developed and tested (i.e. verified), systems integration and testing were conducted. This was done first on veroboard and afterwards with the assistance of a CAD model to ensure structural fit before PCBs were manufactured. Each of these functional units was tested for validity. This is discussed in the next chapter.

CHAPTER 5: EMPIRICAL TESTS AND RESULTS

5.1 INTRODUCTION

Evaluation was done according to Figure 2-10 on page 24. Verification was done as a continuous process which commenced during the first iteration of the design phase in the DSR methodology, and extended through to evaluation (essentially, validation) in the environment. The specific requirements for test and evaluation (verification) were defined during the needs analysis in the conceptual design phase on page 32.

5.2 TEST 1: RECORD COSMIC-RAY ACTIVITY

5.2.1 Pulse detection

The purpose of this test is to show that the functional requirement set in Section 3.2.3 page 34 is met to the specification set in the performance requirements.

Two controlled experiments were conducted. The first (Part A) was to show that the amplifier is operating correctly. The second (Part B) was to show that the MNM-DAS can process incoming pulses at a rate of more than 1500 pulses per second.

5.2.1.1 Part A

The energy spectrum of a proportional counter tube can be seen with a pulse-height analysis since the height of the pulse is proportional to the energy of the particle. Knowing what the pulse distribution should be will also indicate the deference between the noise and the pulses.

The production model of the MNM-DAS was installed at the SANAE Base with three NM64 counter tubes. The MNM-DAS system replaced the previous registration system running on the base. Using a built-in function of the MNM-DAS, a pulse-height analysis

was conducted to show that the amplifiers are operating to specification. The installation setup can be seen in Figure 5-1.

The discrimination level started on 2.2 V and decreased with 0.14 V every 30 minutes until it reached 0.55 V.

Figure 5-1: Amplification experimental setup

The result of the pulse height analysis is shown in Figure 5-2.

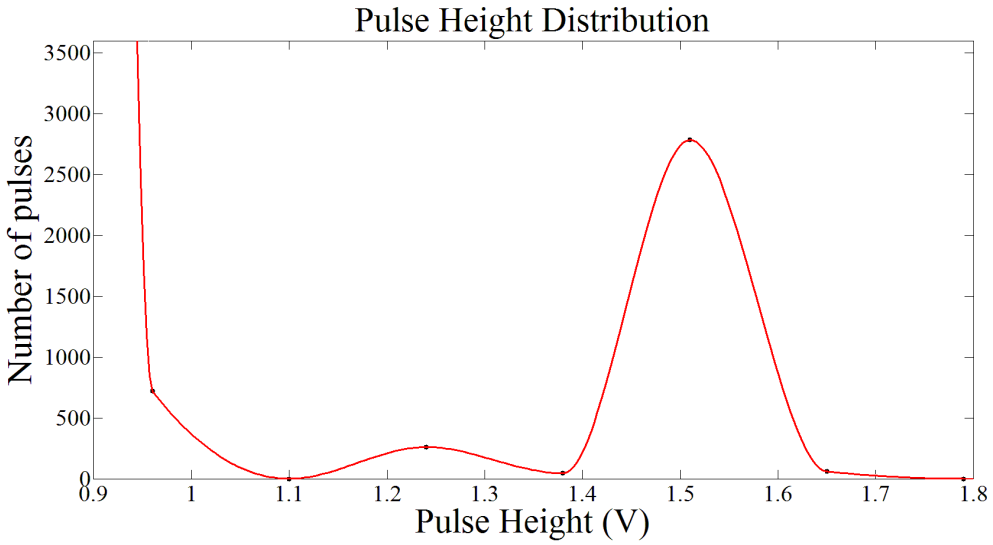

Figure 5-2: Pulse-height distribution

The separation of the noise level and the incoming pulse train can be seen in Figure 5-2. The figure also provides valuable setting information. From this graph, the user can determine exactly where the optimal level is for placing the discriminator level without losing data or introducing noise pulses into the system. For the case shown in Figure 5-2, it is seen that the discrimination level should be set to 1.1 V as all pulses with a higher amplitude than 1.1 V are from reactions inside the proportional counter tube.

5.2.1.2 Part B

To show that the MNM-DAS could achieve a pulse rate of higher than 1500 pulses per second, the pre-amplifier was replaced by a signal generator. This experiment revealed that the MNM-DAS system can receive and process an incoming pulse train of up to 30000 pulses per second before the MNM-DAS misses pulses. This is above the required specification.

5.2.2 Generate high voltage

The purpose of this experiment is to show that F/U 1, the high-voltage supply shown in Figure 4-2 on page 41, meets the functional and performance requirements set out in the

need analysis on page 32. This unit must be able to generate high voltage with a maximum ripple voltage of less than 10 Vp-p.

The experimental setup is the same setup used in Section 5.2.1. In order to operate the NM64 tubes in their proportional region, the high voltage was set to 2850 V. Ten thousand samples were taken every second. The result of this experiment is shown in Figure 5-3.

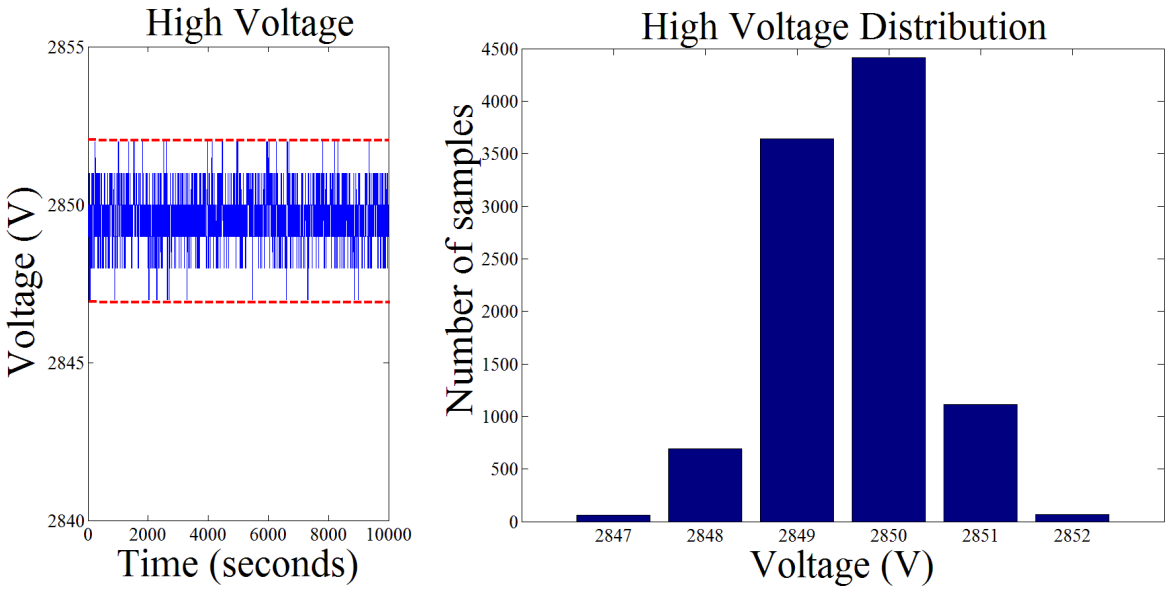

Figure 5-3: High-voltage performance results

From these two graphs, it is clear that the maximum ripple voltage requirement set in the need analysis has not been exceeded. The high-voltage supply produced a ripple voltage of 5 V_{p-p} when the maximum ripple allowed is 10 V_{p-p}.

From the distribution in the graph, it is also evident that the high-voltage density distribution falls within the limits of the specification.

5.2.3 System real-time

The GPS unit (LEA-6/ NEO-6) chosen for this application provides GPS time with a maximum accuracy of 15 ns, but this depends on the satellite coverage. The micro-controller uses its own internal clock for time-keeping and updates its time on a free-

wheeling basis using the GPS as reference (real time is synchronised when major differences are measured). Two ADM MNM-DAS systems were run in parallel as shown in Figure 5-4 for two months.

Figure 5-4: System timing experiment

The MNM-DAS showed a drift of up to two seconds in three days if the firmware does not correct for drift. With the implementation of drift correction, the production version of the MNM-DAS systems has not drifted more than a second over a six–month period. The system time stamps data at a resolution of 1 ms.

5.3 RECORDING OF ENVIRONMENTAL VARIABLES

5.3.1 Atmospheric pressure

The Paroscientific pressure sensor has an accuracy of 0.0001 mbar for the range of 0 to 1000 mbar and can be set to take pressure readings every second. This exceeds the

functional and performance requirements necessary and the specification was met by means of component selection.

5.3.2 Temperature

The needs analysis required that temperature should be recorded to within 1 °C accuracy. To show that the system is capable of operating within specification, the following experiment was conducted. The MNM-DAS recorded temperature in parallel with two calibrated temperature sensor with an accuracy of 0.5 °C each. The sensors were placed in a refrigerator at -15 °C and then heated to 30 °C. A photograph of the experiment is shown in Figure 5-5. The results of the experiment are shown in Figure 5-6. From this graph it is evident that the three sensors had different reaction times to temperature; however, this is not a problem as they all converge once they have settled.

Figure 5-5: Temperature experiment

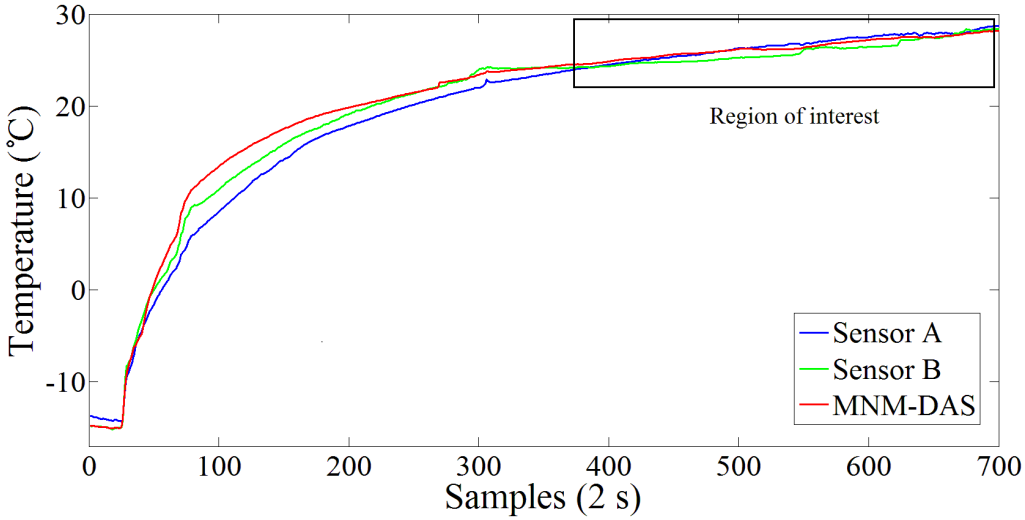

Figure 5-6: Temperature experiment results

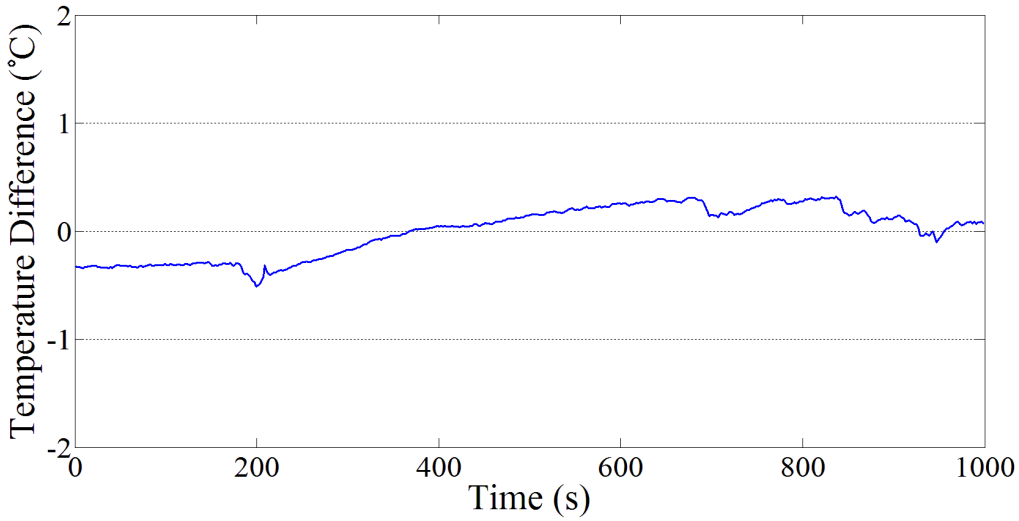

Figure 5-7: Temperature difference

Once the temperature is stable the MNM-DAS temperature sensor does not deviate more than 0.7℃ from the average of the other two sensors. Figure 5-7 shows the difference in temperature between the MNM-DAS and the average of sensors A and B once the temperature has settled at 21℃.

5.3.3 Location

The GPS unit (LEA-6/ NEO-6) chosen for this application provides location information to within five m, exceeding the required accuracy.

5.4 DATA AVAILABILITY

5.4.1 Push data to FTP server

THE ADM and EDM use FTP as a primary data access service. All data shown in this thesis is data collected from the FTP server. Therefore, the FTP functionality is shown to be operationally capable.

5.4.2 Secondary data backup

The ADM model stored a duplicate copy of FTP data onto a flash drive. This was changed with the EDM. The EDM stores data only if there is a fault on the communications (FTP service support) network. This was tested by disabling the Ethernet connection (hence, the FTP support network failure) to test the backup storage function. The secondary storage method worked perfectly. After the network had been connected again the MNM-DAS established a new FTP session and continued storing data on the server. There is a five-second overlap of data to ensure no data is corrupted during a network failure.

5.5 FAULT DETECTION

Fault detection was tested by disconnecting and reconnecting a functional unit or interface. The results can be seen in **Table 5-1**:

Functional unit	Fault detected
F/U 4 & 5: GPS system connected and locked-on	Yes
F/U 10 & I/F 7.2: FTP server operational	Yes
F/U 7: Pressure sensor operational	Yes
F/U 11: USB drive operational	Yes

Table 5-1: Fault detection

The experiment showed that the MNM-DAS could detect failures of the critical functional units.

5.6 EVALUATION

Performance requirements	
P/R 1	Addressed by means of design and component selection
P/R 2	Addressed by means of design and verified in data sets
P/R 3	Demonstrated in Figure 5-7 with experimental verification
P/R 4	Addressed by means of design and verified in data sets
P/R 5	Addressed by means of design and component selection
P/R 6	Demonstrated in Figure 5-3 with experimental verification
P/R 7	Demonstrated in Figure 5-2 with experimental verification
P/R 8	Addressed by means of design and verified in data sets
P/R 9	Addressed by means of design and component selection

Table 5-2: Performance requirements

Functional Requirements	
F/R 1	Demonstrated in Figure 5-2 with experimental verification
F/R 2	Demonstrated in Figure 5-3 with experimental verification
F/R 3	Demonstrated in Figure 5-3 with experimental verification
F/R 4	Addressed by means of design and verified in data sets
F/R 5	Addressed by means of design and verified in data sets
F/R 6	Addressed by means of design and verified in data sets
F/R 7	Addressed by means of design and verified in data sets
F/R 8	Addressed by means of design and verified in data sets
F/R 9	Demonstrated with experimental verification
F/R 10	Addressed by means of design

Table 5-3: Electronic control unit MCDM score

Operational requirements	
O/P 1	Demonstrated in Figure 5-2 with experimental verification
O/P 2	Addressed by means of by design and verified in data sets and demonstrated in Figure 5-6 with experimental verification
O/P 3	Addressed by means of by design
O/P 4	Addressed by means of by design and demonstrated with experimental verification

Table 5-4: Electronic control unit MCDM score

5.7 SUMMARY

This chapter described all the empirical tests that were conducted and their corresponding results. It concluded the evaluation (verification) section of this dissertation and showed that the MNM-DAS met all the performance, functional and operational requirements set out in Section 3.2.

CHAPTER 6: CONCLUSION

6.1 OVERVIEW

The need for an MNM-DAS was identified by the CSR in 2010. In this research, the need was analysed to determine the high-level requirements for the MNM-DAS. Using a systems-engineering approach embedded in a DSR methodology, a conceptual design was extracted from the existing system to describe a generic neutron monitor functionally. This abstracted architecture was then further analysed to ensure that all requirements were addressed before preliminary and detail designs commenced.

The architecture served as input to the preliminary design, which defines the MNM-DAS in more functional detail and defines all interfaces between functional units.

Each functional unit described in the preliminary design was designed, built and tested individually, after which they were integrated and tested as a unit. The integration of all these components yielded the advanced development model (ADM) model; which was thoroughly verified in a laboratory environment before it was installed on a German research vessel, the Polarstern, in December 2011, followed by an installation on a German Antarctic research station, Neumayer III, in January 2012.

While the ADM model continued to operate, an engineering development mode (EDM) was developed to provide solutions to shortfalls of the ADM. The EDM replaced the ADM on the Polarstern in May 2013, and Neumayer III in December 2013. An additional EDM has since also been transported to Mexico to be placed at 4200 m above sea level in conjunction with the High-Altitude Water Cerenkov (HAWC) experiment..

Based on the design of the EDM, a production model was developed. Production started in August 2013 to replace the NM64 registration system at the SANAE Base in January 2014.

The EDM and production models are currently still in operation and are collecting data. The Tsumeb, Potchefstroom and Hermanus stations operated by the CSR are scheduled to be upgraded with the production model before the end of 2015.

6.2 DISCUSSION OF RESULTS

Experiments and results in Chapter 5 showed that all operational, functional and performance requirements set out in the needs analysis were met. Through empirical tests and experiments, the MNM-DAS showed that it was capable of detecting and recording cosmic-ray activity along with all relevant environmental variables.

With the upgrade of the SANAE NM64 monitor, the MNM-DAS showed that it was capable of replacing the recording system for the NM64 neutron monitors.

Thus, with the successful implementation of the MNM-DAS on a calibration monitor body and a NM64 tube, the research question posed by the CSR, namely to

> *develop a system that is capable of being used as a neutron monitor, using the existing hardware of the calibration monitor, and serve as a replacement for the NM 64*

was addressed and validated. The system has shown that it is functionally capable of performing all tasks defined by the initial NM64 monitor, and meets all requirements as set out in the research question.

6.3 SPECIFIC CONTRIBUTIONS

There are three major contributions made towards the body of knowledge in this study, as discussed below:

1. A new methodology that embeds systems engineering (SE) into design science research (DSR) to add structure to the design process that forms part of DSR. This, in turn, speeds up the design process and ensures that all requirements of the

environment (i.e. real world) are addressed in the process of performing applied research;

2. An abstraction of a neutron monitor was created that can be used in future development on the MNM-DAS, or any other neutron monitor that makes use of a similar architecture. This abstraction was successfully applied in this research to direct the design process and provide a design reference framework;
3. The final contribution is in the form of actual artefacts, including all the necessary documentation, to replace an out-dated artefact. The final artefact, a production model, is of modular design and has been validated by its successful application in a real-world environment. Using the above abstraction, it will be possible to replace or upgrade any functional unit individually if necessary in the future.

6.4 VERIFICATION AND VALIDATION

Verification of this research work was achieved as follows:

1. All requirements of the initial system were extracted, documented, and accepted as being sufficient by the CSR. The requirements were provided in Chapter 3;
2. Requirements were addressed by means of a formal design process, where all requirements were adhered to in the form of a functional (abstract) design;
3. The physical design (artefact), was rigorously verified (tested) by performing controlled tests in a laboratory environment;
4. Functional capability of individual units, as well as capability of the integrated artefact, was demonstrated and verified.

The above verification evidence shows that the research requirement for verification has been met.

Also, in doing the above, the application of an integrated DSR and SE process was shown to be effective in the research and development of an MNM-DAS. Thus, the research and development process was validated.

Final validation of the research work was achieved by implementing the MNM-DAS artefacts in real-world applications. Neutron measurement results from the MNM-DAS have been used to provide neutron counting data to the international space research community, and the ADM, EDM and production models have all been successfully applied in practice.

6.5 CONCLUSION AND PROPOSED FUTURE WORK

6.5.1 Conclusion

This dissertation described the research and development of a mini-neutron monitor data acquisition system (MNM-DAS). An existing monitor was used as design reference, and all requirements used as input to the new system were extracted, validated and utilized throughout this research. The MNM-DAS was successfully designed and developed by following a systems engineering approach embedded in a design science research framework. The MNM-DAS was constructed and tested, and is currently being used in real-world applications internationally.

6.5.2 Proposed future work

The abstract model provides a framework for future research and development. Currently, an autonomous neutron monitor is under development that already references the abstract model. This autonomous monitor will be capable of operating in extreme environments, a challenge not present in the MNM-DAS development. In such extreme environments, the monitor will be placed in remote locations where temperatures may reach levels as low as -40 °C. As a result, the new monitor must use minimal power and must be able to withstand extreme environmental conditions.

The work done in this research serves as input into the new development and will definitely aid in the successful and speedy development of new artefacts.

APPENDIX A

Centre for Space Research

Neutron Monitor User Manual

NORTH-WEST UNIVERSITY ®
YUNIBESITI YA BOKONE-BOPHIRIMA
NOORDWES-UNIVERSITEIT

May 2013

Revision 1.2

THE MINI NEUTRON MONITOR

Physical Inspection

You should have received the following items with your Mini-neutron monitor

- Standard mini neutron monitor electronics head.
- User's manual.
- 16GB flash drive.
- Micro USB power adapter.
- RJ11 to DB9 converter.
- Passive GSP antenna.

6.5.3 Display

The front panel contains the display, keypad and various light indicators. The display shows the following list of information.

- Current date.
- Current UTC time.
- Neutron counts since startup.
- Pressure.
- Temperature.
- High voltage.
- USB flash drive status.
- Uptime.

↑ ↓ Use the up and down arrow keys to navigate the display.

The light indicators show the following from top to bottom

- Processor running.
- GPS status.
- Network status.
- Flash drive status.
- Pressure status.

Front display

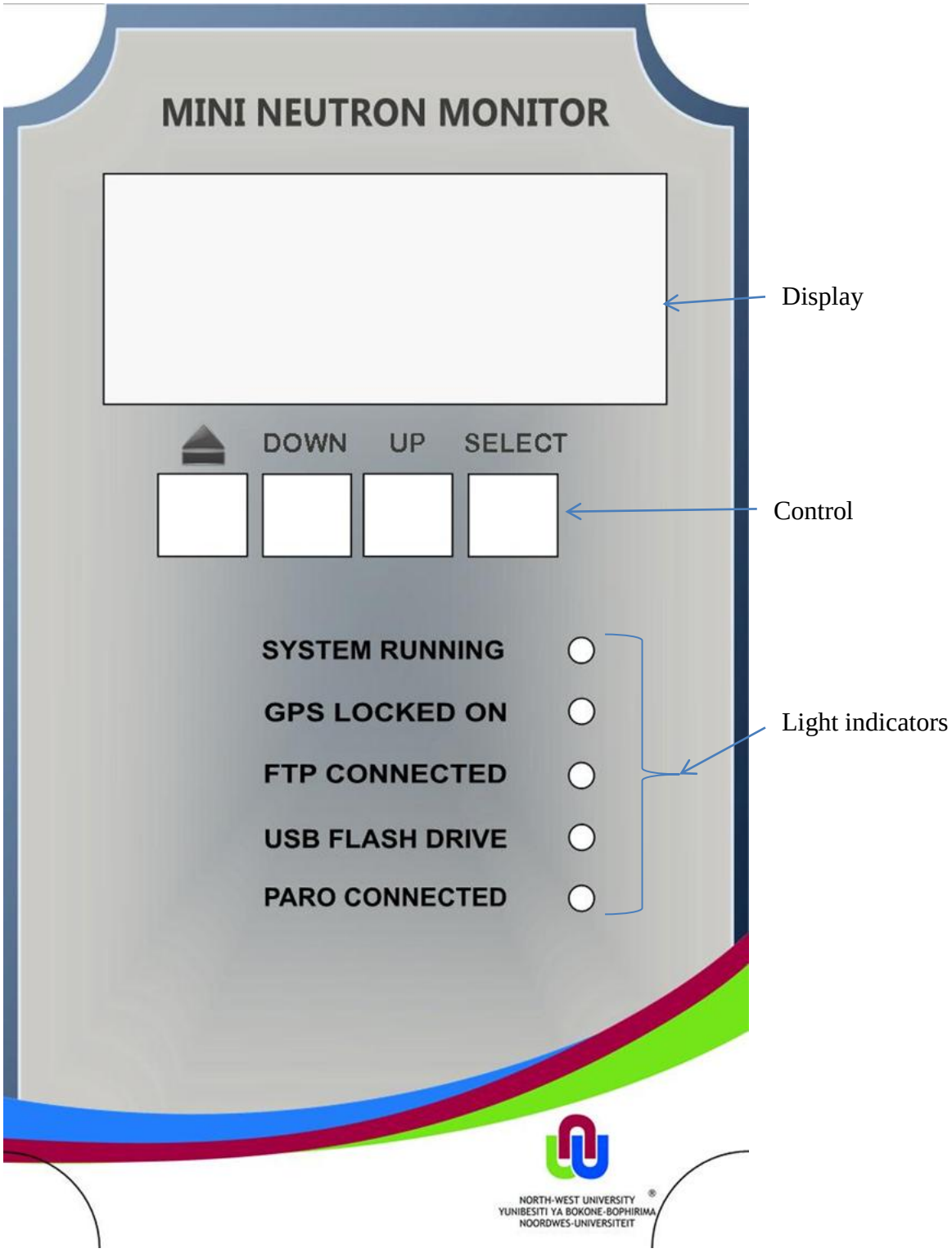

INSTALLING YOUR MINI NEUTRON MONITOR

Step 1

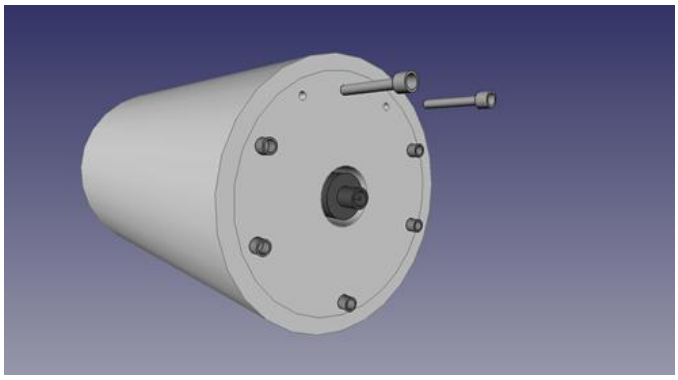

Step 2

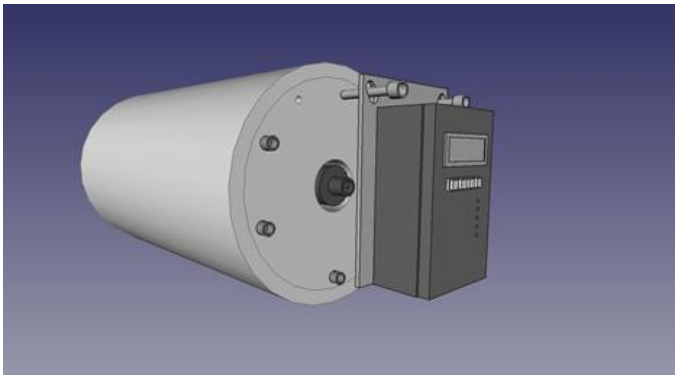

Step 3

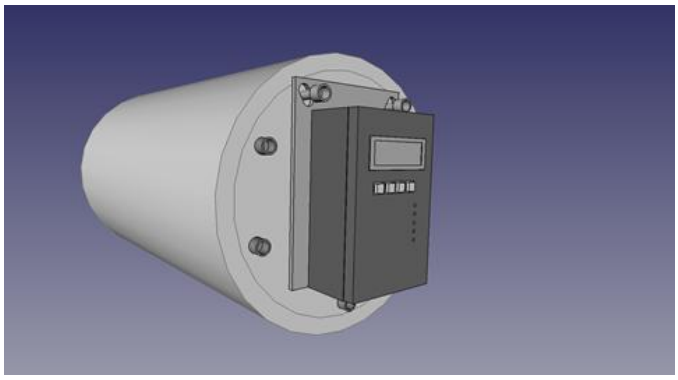

Step 4

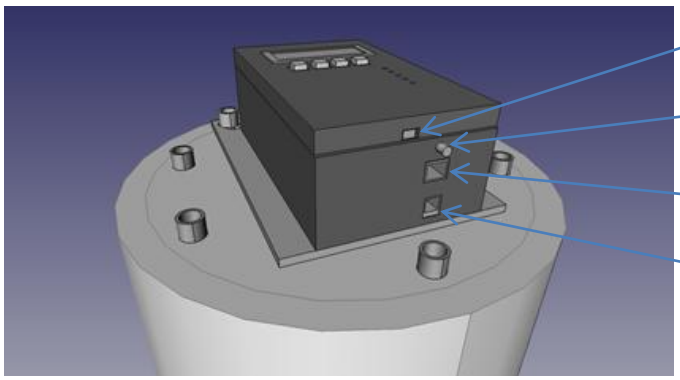

Unscrew the top two nuts on the monitor body. Connect the counter tube to the back of the electronic box. Gently slide the counter tube into position lining up the holes in the back plate with the top two holes on the monitor body. Place the nuts back into position and tighten.

Connect the GPS passive antenna the bottom of the electronics head. Connect the Ethernet cable to the corresponding RJ45 socket at the bottom. Finally connect the power cable to the bottom of the electronic box and turn on the power.

Optional: Connect the serial cable to the registration PC if further backup is required. Use the supplied RJ11 to DP9 converter cable supplied.

Once turned on, you should see a welcome screen with the version of the firmware. The processor running light should start flashing. Press the up or down arrow button to start navigating your display.

The data registration will only begin when GPS lock is obtained, indicated by the 2nd light. The 3rd light indicates whether the flash drive has been successfully mounted. Once GPS lock is obtained, the monitor will establish network connection by using the configuration file supplied on the flash drive.

Successful connection of the Paroscientific pressure sensor is indicated by the 5th light.

As soon as the FTP connection to the server is established the 4th light will turn on indicating data is being transferred to the FTP server.

USER INTERFACE

6.5.4 Network configuration

The network configuration is set by editing a text file (config.txt) in the root of the registration flash drive. See the following example

FTP_IP:192.168.5.90; (No Spaces should be present)
Username:muonic;
Password:Astro11*;
Monitor_tube_number:POL1;
Monitor_IP:192.168.5.91;
Monitor_Sub_net:255.255.255.0;
Please note that changes to this file will only take effect once the system has been restarted.

6.5.5 USB flash drive configuration

← When you need to remove the flash drive press the eject button in order to un-mount the flash drive. Once the drive has been un-mounted the USB indicator light will switch off and it will be safe to remove the drive. Failure to un-mount the flash-drive can cause loss of data.

It is important to note that the file system on flash drive should be FAT32.

6.5.6 Serial connection configuration

The serial connection runs a baud rate of 19200 bits per second. Hardware flow control set to none and one stop bit.

The ***Qgraph*** registration software will handle the setup in the background, only the correct com port should be selected.

CONTACT DETAILS

nmsupport@nwu.ac.za

BIBLIOGRAPHY

[1] H. Moraal and P. H. Stoker, "Long-term neutron monitor observations and the 2009 cosmic ray maximum," *Journal of geophysical research*, vol. 115, no. A12109, pp. 0148-0227, Dec. 2010.

[2] H. Krüger, "A calibration neutron monitor for long-term cosmic ray modulation studies," M.Sc Thesis, North-West University, Potchefstroom, 2006.

[3] H. Moraal, A. Belov, and J. M. Clem, "Design and co-ordination of multi-station international neutron monitor networks," *Space Science Reviews*, vol. 93, pp. 285-303, Jun. 2000.

[4] H. Krüger and H. Moraal, "A calibration neutron monitor: Statistical accuracy and environmental sensitivity," *ScienceDirect*, vol. 46, pp. 1394-1399, Jul. 2010.

[5] H. Krüger and H. Moraal, "Neutron monitor calibrations: progress report," North-West University, 2013.

[6] G. Brooke and A. W. Wolfendale, "The momentum spectrum of cosmic ray protons near sea level in the momentum range 0.6-150 GeV/c," *Proceedings of the Physical Society*, vol. 83, no. 5, pp. 843-851, 1964.

[7] P. H. Stoker, L. I. Dorman, and J. M. Clem, "Neutron monitor design improvements," *Space Science Reviews*, vol. 93, pp. 361-380, Jun. 2000.

[8] E. F. Minnie, "Technology roadmap for improvement of the North-West University neutron monitor system of the Centre for Space Research," North-West University M.Eng, 2010.

[9] H. Krüger and H. Moraal, "A calibration neutron monitor: Statistical accuracy and environmental sensitivity," *Advances in Space Research*, vol. 46, pp. 1394-1399, Jul. 2010.

[10] H. Mavromichalaki, et al., "Applications and usage of the real-time neutron monitor database," *Advances in Space Research*, vol. 47, no. 12, pp. 2210-2222, 2011.

[11] G. F. Knoll, *Radiation Detection and Measurement*. United States of America: John Wiley & Sons, 1979.

[12] A. R. Hevner, S. T. March, and J. Park, "Design science in information systems research," *MIS Quartely*, vol. 28, no. 1, pp. 75-105, Mar. 2004.

[13] G. l. Geerts, "A design science research methodology and its application to accounting information systems research," *International Journal of Accounting Information Systems*, vol. 12, pp. 142-151, Feb. 2011.

[14] A. Hevner and S. Chatterjee, *Design Research in Information Systems Theory and Practice*. 2010.

[15] A. Kossiakoff, W. N. Sweet, S. J. Seymour, and S. M. Biemer, *Systems Engineering Principles and Practice*, second edition ed. John wiley & Sons, 2010.

[16] K. R. Fowler, *Electronic instrument design architecting for the life cycle*. New York:

oxford university press, 1996.

[17] E. Kuffel, W. S. Zaengl, and J. Kuffel, *High Voltage Engineering Fundamentals*, Second edition ed. Butterworth-Heinemann, 2000.

[18] S. Strachan, "Synthesis and evaluation of a charge sensitive amplifier for neutron counters," Ming Thesis, North-West University, Potchefstroom, 2013.

[19] B. Kuechler and V. Vaishnavi, "On theory development in design science research: anatomy of a research project," *Journal of Information Systems*, vol. 17, pp. 489-504, Sep. 2008.

[20] J. M. Clem and L. I. Dorman, "Neutron monitor response functions," *Space Science Reviews*, vol. 93, no. 1-2, pp. 335-359, 2000.

[21] B. S. Blanchard and W. J. Fabrycky, *Systems Engineering and Analysis*, T. Edition, Ed. New Jersey: Prentice hall, 1997.

[22] S. Gregor and A. R. Hevner, "Positioning and presenting design science research for maximum impact," *MIS Quarterly*, vol. 37, no. 2, pp. 337-355, Jun. 2013.

[23] J. A. Simpson, "The cosmic ray nucleonic component:the invention and scientific uses of the neutron monitor," *Space Science Reviews*, vol. 93, pp. 11-32, Apr. 2000.

[24] H. Moraal. (2014, Mar.) Centre for Space Research. [Online]. http://www.nwu.ac.za/neutron-monitor-data-0